

Lawrence Berkeley National Laboratory

LBL Publications

Title

Studies in Beta and Gamma Ray Spectroscopy

Permalink

<https://escholarship.org/uc/item/2b3156pc>

Author

Hayward, Raymond Webster

Publication Date

2024-03-06

UNCLASSIFIED

UCRL-582

Copy 1

STUDIES IN BETA AND GAMMA RAY SPECTROSCOPY

by

Raymond Webster Hayward, Jr.
B.S. (Iowa State College) 1943

DISSERTATION

Submitted in partial satisfaction of the requirements for the degree of

DOCTOR OF PHILOSOPHY

in

Physics

in the

GRADUATE DIVISION

of the

UNIVERSITY OF CALIFORNIA

Approved:

.....
.....
.....

Committee in Charge

DISCLAIMER

This document was prepared as an account of work sponsored by the United States Government. While this document is believed to contain correct information, neither the United States Government nor any agency thereof, nor the Regents of the University of California, nor any of their employees, makes any warranty, express or implied, or assumes any legal responsibility for the accuracy, completeness, or usefulness of any information, apparatus, product, or process disclosed, or represents that its use would not infringe privately owned rights. Reference herein to any specific commercial product, process, or service by its trade name, trademark, manufacturer, or otherwise, does not necessarily constitute or imply its endorsement, recommendation, or favoring by the United States Government or any agency thereof, or the Regents of the University of California. The views and opinions of authors expressed herein do not necessarily state or reflect those of the United States Government or any agency thereof or the Regents of the University of California.

STUDIES IN BETA AND GAMMA RAY SPECTROSCOPY

by

Raymond Webster Hayward, Jr.

Introduction

The study of artificial radioactive isotopes is at the present time one of the most important topics in nuclear research. It involves the establishment of a detailed term scheme for the disintegration in question. Not only are the energies of the components of the different beta and gamma radiations of interest, but also their intensities. These data give information concerning the probabilities of transitions between the different nuclear energy levels. From them it is possible to draw conclusions regarding the mechanism of the disintegration and to correlate the spins and parities of the levels.

The theoretical basis for such considerations is at present in an uncompleted stage, and development in the theoretical field is hindered by the fact that term schemes for relatively few disintegrations have been established experimentally. There have been a large number of investigators who have made observations with absorption techniques alone, most of which are open to question, especially if there is any complexity in the disintegration scheme. Far fewer have been the number of investigators using beta-ray spectrometers. A rather comprehensive list of observers may be found in the Table of Isotopes of Seaborg and Perlman.¹

The detailed experimental results of beta-ray emission are usually interpreted in terms of a theory which was in its simplest form developed by Fermi² on the basis of the neutrino hypothesis, but the theory

is capable of many variations and can consequently be made to agree with a wide range of different experimental results. A full discussion of beta-decay theory was given by Konopinski.³ Only the minimum amount necessary to serve as a basis for the discussion and interpretation of experiments will be given here.

The theory proceeds directly from the quantum mechanical expression for the rate of transition processes from a given quantum state to another where the assumption is made that the energy and momentum are shared between the electron and a neutrino of zero rest mass as well as the residual nucleus. Then Fermi's equation for the probability per unit time that a nucleus will emit an electron (or positron) of momentum in the interval between p and $p + dp$ is

$$P(p) dp = G^2/(2 \pi^3) |M|^2 F(Z,p) p^2 (W_0 - W)^2 dp$$

where p and W are the momentum and energy of the electron in units of mc and mc^2 respectively, and W_0 is the maximum energy of the beta spectrum. $W_0 - W$ represents the momentum (and also the energy) of the neutrino. $F(Z,p)$ represents the effect of the Coulomb field of the nucleus on the beta-particle. $G^2/2 \pi^3$ is a constant determined empirically representing the magnitude of the interaction between nucleons and the electron-neutrino field. The factor $|M|^2$ represents the square of the absolute value of the matrix element containing the form of the interactions and wave functions characteristic of the initial and final states of the nucleus. For allowed transitions this factor is of the order of unity and for forbidden transitions it has smaller values and may sometimes be a function of the energy of the electron and the neutrino.

The essential difficulty in the beta-decay theory is to guess the

kind of interaction between the heavy particle and the light particles (beta-particle and neutrino). It could be any one of five relativistically invariant types, namely: scalar (S), polar vector (V), tensor (T), axial vector (A), and pseudoscalar (P). On the basis of experimental results the interaction currently in vogue is the tensor interaction, which gives rise to the so-called Gamow-Teller selection rules.⁴ There is an additional selection rule due to Wigner⁵ which makes some allowed transitions favored over others if the space wave functions of the initial and final states are similar. If there is a substantial change in the space wave functions (change in symmetry or configuration), the transition may still be allowed but with a reduced nuclear matrix element. The selection rules for each of the above interactions are found by expanding the matrix elements. Then for each term the operator has to be chosen so that only those transitions occur for which the angular momentum and the parity of the system are conserved. Selection rules resulting for each of these interactions are tabulated below.

Interaction	Allowed	1st forbidden	2nd forbidden
S ΔI parity change	0 no	$0, \underline{+1}$ no $0 \rightarrow 0$ yes	$\underline{+1}, \underline{+2}$ no $1 \rightarrow 0$ no
V ΔI parity change	0 no	$0, \underline{+1}$ no $0 \rightarrow 0$ yes	$\underline{+1}, \underline{+2}$ no
T ΔI parity change	$0, \underline{+1}$ no $0 \rightarrow 0$ no	$0, \underline{+1}, \underline{+2}$ no $0 \rightarrow 0$ yes	$\underline{+2}, \underline{+3}$ no
A ΔI parity change	$0, \underline{+1}$ no $0 \rightarrow 0$ no	$0, \underline{+1}, \underline{+2}$ no $0 \rightarrow 0$ yes	$\underline{+2}$ no
P ΔI parity change	0 yes	$0, \underline{+1}$ no $0 \rightarrow 0$ no	$\underline{+1}, \underline{+2}$ no $1 \rightarrow 0$ yes

If the selection rules require that the first term in the expansion of the matrix element be equal to zero so that the second term is the first nonvanishing term, then the transition is referred to as first forbidden and so on. First forbidden transitions should be smaller by a factor of about 10^{-2} since the successive terms in the expansion are smaller than the preceding by the factor $\bar{p}R/\hbar$ where \bar{p} is the average momentum and R is the nuclear radius in units of \hbar/mc . Accordingly each higher degree of forbiddenness is smaller by a factor of 10^{-2} .

The decay constant for a particular transition is given by

$$1/\tau = \int_0^{P_{\max}} F(p) dp = G^2/2 \pi^3 f(Z, W_0)$$

where

$$f(Z, W_0) = \int_0^{P_{\max}} F(Z, W) p^2 (W_0 - W)^2 dp.$$

$f(Z, W_0)$ is a function only of the charge and the upper energy limit and hence can be calculated for any element for which these quantities are known. The product of f and τ which can be determined experimentally gives the magnitude of the term $G^2/2 \pi^3 |M|^2$ and hence enables one to classify beta activities experimentally into their order of forbiddenness as the value $f\tau$ will fall into groups differing by a factor 100.

The upper energy of the beta spectrum is found by an ingenious method of presenting the data, first proposed by Kurie.⁶ If one observes in a magnetic lens spectrograph the number of electrons in a momentum interval Δp , which is proportional to $F(p) \Delta p$, then the number observed is

$$N(p) = G^2/2 \pi^3 |M|^2 F(Z, p) p^2 (W_0 - W)^2 \Delta p.$$

Now for a given type of interaction $|M|^2$ is a constant as well as

$G^2/2\pi^3$ and the resolving power of the spectrograph Δp is proportional to the momentum measured, which is in turn proportional to the magnetic field, H , and hence the current. One can write the number of electrons obtained for a given current value as

$$N(I) = \text{const } F(Z, I) I^3 (W_0 - W)^2.$$

Thus if one plots $\sqrt{N(I)}/[I^3 F(Z, I)]$ as a function of W , one should obtain a linear function with an intercept at $W = W_0$. This method requires accurate knowledge of the function $F(Z, p)$ which is nothing but the Dirac wave function for a charged particle in a Coulomb field when the particle is in an unbound state (i.e. in a continuum). It is

$$F(Z, p) = \frac{4 (2pR)^{2s-2} e^{\pi aZW/p} |\Gamma(s + iaZW/p)|^2 \cdot (s+1)}{|\Gamma(2s+1)|^2 \cdot 2}$$

where p , W , Z and R are the same quantities and in the same units as before, a is the fine structure constant, and $s = (1 - a^2 Z^2)^{1/2}$.

$F(Z, p)$ is difficult to calculate since there are no good tables of the complex gamma function. However, it is possible to approximate the function to any degree of accuracy by expressing the gamma function as an infinite product. For very light nuclei ($Z < 15$) where $s \approx 1$ one can make use of identities for the Γ function to get

$$F(Z, p) = \text{const} \frac{2\pi aZW/p}{1 - e^{-2\pi aZW/p}}$$

Bethe⁷ gives the approximation that is good within a few percent for all values of Z

$$F(Z, p) = \text{const} \frac{2\pi aZW/p}{1 - e^{-2\pi aZW/p}} [W^2 (1 + 4a^2 Z^2) - 1]^{s-1}.$$

Longmire and Brown⁸ give corrections to be made for the screening of the nuclear charge by the atomic electrons which are negligible for

electron emission but quite appreciable for positrons emitted with energies less than 100 Kev.

The study of beta spectra is complicated by the secondary effects which always appear to a smaller or greater extent in the form of scattering from the backing of the sample and the sample itself and scattering from the internal surfaces of the spectrometer. This effect manifests itself in the fact that the number of low energy electrons relative to the remainder of the spectrum increases. This phenomenon is frequently so marked that simple spectra give Fermi plots so curved that they have been falsely interpreted as having several components. The best precautionary measure against these disturbing effects is to use samples of high specific activity spread over a large area with a backing and covering of as low a mass as possible. In the recording of continuous spectra it is unnecessary to work with high resolving power. The Fermi plot obtained for infinite resolving power will coincide with that for a finite resolving power except in the region very near the end point, and if no importance be attributed to the last points in a Fermi plot, it is unnecessary to introduce a correction. This is, however, not the case if it is desired, for example, to determine the energy maximum by a direct study of the end point of the original spectrum, but this is not usually feasible because of the very low intensity near the end point.

The experimental fact that most allowed and forbidden beta spectra may be represented as straight lines in the Fermi analysis facilitates the resolution of complex spectra into their components. However, it should be pointed out that the resolution of a spectrum into its components may often be difficult to perform especially when the lower

energy components are also low in intensity since back scattering by the more intense components may simulate the low energy components. However, this method of analysis usually allows the end points of the low energy components to be found with reasonable accuracy. When two or more components originate from the same level there is always the additional information gained from the investigation of the gamma-radiation since the difference in the energy of the beta components must occur in the form of gamma-radiation. The energies of the latter when known may be employed in the Fermi analysis.

It often occurs that the beta transitions to different excited levels in the final nucleus are so strongly forbidden by selection rules that they are completely absent. Even the beta transition to the ground state of the final nucleus may be so forbidden that the final state can be reached only by gamma emission from some higher excited state.

A nucleus in an excited state can decay to a lower energy state of the same nucleus by either emitting a gamma-ray of energy $h\nu$ equal to the energy difference between the two states or by giving the energy to an electron in the K, L, ... shell of the same atom, the electron being ejected with kinetic energy $W_\gamma - E_K$, $W_\gamma - E_L$ etc., where E_K , E_L ... are the binding energies of the electrons in their respective shells. This latter process is called internal conversion and is not a secondary process but a primary one and is due to the direct interaction of the nucleus with the surrounding electrons. This is important for it means that the probability of decay of the excited state is not simply the probability of gamma emission but is the sum of the probabilities of the two competing processes of gamma emission and internal conversion.

Unlike the theory of beta-decay the theory of gamma radiation and internal conversion is rather well understood and is treated in a number of places, e.g., Dancoff and Morrison.⁹ Essentially the quantum theory of gamma-ray emission utilizes the classical conception of a radiation source as an oscillating electric or magnetic multipole but replaces the rate of radiation of energy of angular frequency ω by $\hbar\omega$ times the probability per unit time that a quantum of energy $\hbar\omega$ shall be emitted. When this theory is subjected to conservation considerations namely, of angular momentum and parity, it gives rise to the selection rules for multipole radiation given below.

Parity	l even	l odd
same	2^l electric 2^{l+1} magnetic	2^{l+1} electric 2^l magnetic
opposite	2^{l+1} electric 2^l magnetic	2^l electric 2^{l+1} magnetic

where $|I' - I| \leq l \leq |I' + I|$ and I' is the spin of the initial state and I that of the final state.

As in beta-decay theory it is not possible to calculate the absolute probability of the transitions without some knowledge of the matrix elements and estimates of these require a nuclear model the details of which are beyond our present knowledge. Segrè and Helmholtz¹⁰ give an approximate formula for the number of quanta emitted per unit time, λ_γ

$$\log_{10} \lambda_\gamma = 20.30 - 2 \log_{10}(1 \cdot 3 \dots 2l - 1) - (2l + 1)(1.30 - \log_{10} W_\gamma) - 2l(0.84 - 1/3 \log_{10} A)$$

where W_γ is the energy of the gamma-ray, l is the multipole order for electric radiation. The decay constant for magnetic 2^l pole radiation may be obtained by inserting $l = l' + 1$. Since internal conversion is

a competing process the effect will increase the decay constant to $\lambda = \lambda_\gamma + \lambda_e$ where λ_e is the decay corresponding to the transition probability induced by electrons. Hence the half-life of an excited state will be

$$\tau_{1/2} = 0.693/(\lambda_\gamma + \lambda_e) = 0.693/\lambda_\gamma (1 + \alpha)$$

where α is the internal conversion coefficient which is defined as the number of conversion electrons per quantum emitted. Curves of half-life versus gamma-ray energy as functions of various multipole orders and conversion coefficients are given in a recent paper of Axel and Dancoff.¹¹

The radiation field due to any given strength of multipole oscillator can be written down and the interaction of such a field with the atomic electrons can be calculated from the known wave functions. Hence the internal conversion coefficient can be calculated independently of the magnitude of the nuclear matrix element but with some assumption about the multipole nature of the transition. Explicit expressions for the internal conversion coefficient applicable to all values of Z , transition energies, and multipole types have not been obtained on account of the mathematical complexities, but calculations have been made with varying degrees of approximation in particular cases. Hebb and Uhlenbeck¹² have obtained nonrelativistic expressions for the K conversion coefficient α_K for electric transitions only, which are not too far off for transition energies $W_\gamma \ll m_0 c^2$ and for $Z < 40$. The calculations have been extended by Dancoff and Morrison⁹ and by Hebb and Nelson¹³ to include magnetic multipole transitions and L conversion. Expressions for the conversion coefficient as given by Dancoff and Morrison for K conversion when the binding energy of the K

-11-

electrons is much smaller than W_γ are

Electric transitions

$$\alpha_K^l = \frac{2Z^3 a^4}{W_\gamma^3} \left(\frac{W_\gamma + 2}{W_\gamma} \right)^{l-1/2} \frac{(\ell + 1)W_\gamma^2 + 4\ell}{\ell + 1}$$

Magnetic transitions

$$\beta_K^l = \frac{2Z^3 a^4}{W_\gamma^3} \left(\frac{W_\gamma + 2}{W_\gamma} \right)^{l+1/2}$$

where W_γ is in units of m_0c^2 and ℓ represents the multipolarity of the transition.

More exact values for the conversion coefficients have been recently calculated by Rose et al.¹⁴ using the automatic computer at Harvard and are published in the form of tables.

Using nonrelativistic wave functions and assuming the wave-length of the gamma-radiation to be much larger than atomic dimensions, Hebb and Nelson obtained the ratio $\frac{\alpha_K}{\alpha_L}$ for both electric and magnetic multipole radiation which are correct to about twenty percent for the experimental cases treated in this paper. Their results will not be listed here because of their complexity.

The investigation of gamma spectra are complicated by difficulties of intensity to a much higher degree than for beta spectra since the efficiencies of the measuring devices are strongly dependent on the energy of the radiation. Compton effect and the photoelectric effect are the most used in the investigation of gamma-radiation with a magnetic lens spectrometer.

When applicable the most convenient and accurate method of determining the energy of the gamma-radiation is by measuring the energy of the internal conversion electrons associated with the same energy

transition. These internal conversion electrons fall into discrete groups, $W_\gamma - E_K$, $W_\gamma - E_L$, etc., the lines separated by $E_K - E_L$ corresponding to the same transition. The high intrinsic accuracy arises from the fact that no secondary radiator is required to convert the gamma-radiation into measurable electrons. The spread of energy depends only on the thickness of the source. Since the internal conversion coefficient is strongly dependent on the type and energy of the gamma-radiation, it is not convenient to use the number of the conversion electrons as an indication of the intensity of the gamma-radiation. However, if the intensity of the radiation can be determined by other means, then the number of conversion electrons can give information on the type of radiation which is valuable in assigning spin and parity values of the levels. Another method of finding the type of radiation, which is independent of the intensity of the gamma-radiation, is to observe the relative number of K conversion electrons to L conversion electrons.

The production of Compton electrons may be achieved by pressing the active sample into a small copper cylinder the walls of which are thick enough to absorb all of the continuous beta-radiation. Owing to the high density of copper the radiator may be made small. For a given diameter of the radiator a larger active quantity of substance can be inserted than if the radiator were of aluminum. At energies above 0.5 Mev only Compton electrons are obtained but below this value the photoelectric effect in copper makes a small contribution.

If a thin foil of high atomic number (e.g., Pb, Au, or U) is placed outside the radiator then photoelectrons from the radiator will be present in addition to the Compton electron spectrum. The photo-

electric effect is especially marked for gamma-radiations of less than 0.8 Mev.

At the higher gamma energies it may be often difficult, especially when gamma components are closely adjacent, to distinguish the contributions of the photoelectric effect from the edges of the corresponding Compton spectrum. The photoconversion lines often manifest themselves in terracings of the high energy side of the Compton distribution which are usually difficult to interpret.

The determination of the gamma energies is especially accurate when the photoelectric effect can be utilized, the high accuracy being due to the fact that the peak of a well defined line is measured. The reliability of the determination is enhanced if not only the K photoconversion line but also the L photoconversion line can be measured. For a given resolving power this condition is fulfilled at low energies of gamma-radiation which are associated with larger intervals between the K and L lines.

In cases where there is a difficulty in utilizing the photoelectric effect the gamma energy may be determined with moderate accuracy by measuring the inflection point at the upper edge of the Compton spectrum obtained before dividing the ordinate by the corresponding abscissa. Siegbahn¹⁵ finds empirically that the value of the energy obtained in this manner, when inserted in the equation for the Compton effect from central impact between a photon and an electron, gives the same gamma energy within the limits of error as that obtained from the K photoconversion line plus the binding energy for the K shell.

An important matter in the analysis of the term scheme for any radioactive disintegration is the relative intensity of the gamma

radiations, since these magnitudes give information regarding the transition probability between the various levels. To find the relative intensities for each gamma-ray the area of the Compton electron distribution must be multiplied by a factor dependent on the energy of the gamma-ray which can be derived from an efficiency curve for the radiation. Siegbahn¹⁶ has developed an empirical method for obtaining this factor within 10 percent.

To form term schemes from information gained by the above methods it is necessary to make definite assumptions regarding the order or sequence of the different components. In many cases this is possible but frequently one encounters difficulty. It is very valuable in this event to employ the coincidence method which makes possible a more direct study of the association between the different beta and gamma components. This method was first used by Deutsch and co-workers.¹⁷ It has since found increasing use notably by Siegbahn and Johansson¹⁸ as the result of improved designs for coincidence amplifiers with considerably improved resolving times. In most coincidence applications it is necessary to study both the gamma-gamma and beta-gamma coincidence effects. In the latter case the beta-gamma coincidence effects can be measured as a function of the spectrally resolved beta energy intervals. This may be illustrated by a simple example. We assume that we have measured a beta spectrum which we assume to be complex in view of the presence of a weak gamma activity of unknown energy. A resolution into beta components by direct Fermi analysis of the complex spectrum would be associated here with great sources of error as a consequence of the weak intensity of the softer component. However, spectral resolution of the beta-gamma coincidence effect will

here presumably have the same form as the softer beta component. By making the Fermi plot for the coincidence spectrum it is possible in this manner to obtain an upper limit of the softer beta component.

The requirements on the resolving time of the coincidence circuit and strength of the sample are much more stringent than in ordinary absorption coincidence applications, since the chance coincidences must be negligible compared to the true coincidences in order properly to resolve the softer beta component. The true coincidence counting rate will be

$$N_{\beta\gamma} = N \epsilon_{\gamma} \epsilon_{\beta}(I)$$

where N is the number of disintegrations per second and ϵ_{γ} the "efficiency" of the gamma-ray counter. The term "efficiency" includes the effective solid angle presented by the counter to the source as well as the actual efficiency of the counter for a particular gamma-ray energy.

$\epsilon_{\beta}(I)$ is the "efficiency" of the beta-ray counter which takes into account the solid angle and true efficiency as well as the fact that only the spectrally resolved portion of the beta spectrum is counted. Hence $\epsilon_{\beta}(I)$ will be proportional to the factor $F(Z, I) I^3 (W_0 - W)^2$. Since the two individual counting rates in the gamma and beta counters are

$$N_{\gamma} = N \epsilon_{\gamma} \quad \text{and} \quad N_{\beta} = N \epsilon_{\beta}(I)$$

the ratio $N_{\beta\gamma}/N_{\beta}$ should be constant and equal to the efficiency of the gamma counter ϵ_{γ} . However, the counting rate observed on the coincidence counter will be the sum of the true and chance coincidence rate, and unless the chance coincidence rate is small compared to the former, the ratio $N_{\beta\gamma}/N_{\beta}$ will not be constant but a function of the beta-particle momentum. The chance coincidence rate is

$$N_{\text{chance}} = 2N_{\beta} N_{\gamma} \tau = 2N^2 \epsilon_{\gamma} \epsilon_{\beta} \tau$$

hence if we require that $N_{\beta\gamma} > 100N_{\text{chance}}$ we have the requirement that $N\tau < 10^{-2}$ which means that the source strength is limited to approximately one or two microcuries for a resolving time of 0.2 microsecond, the resolving time of the coincidence circuit used in the experiments treated in this paper.

Apparatus

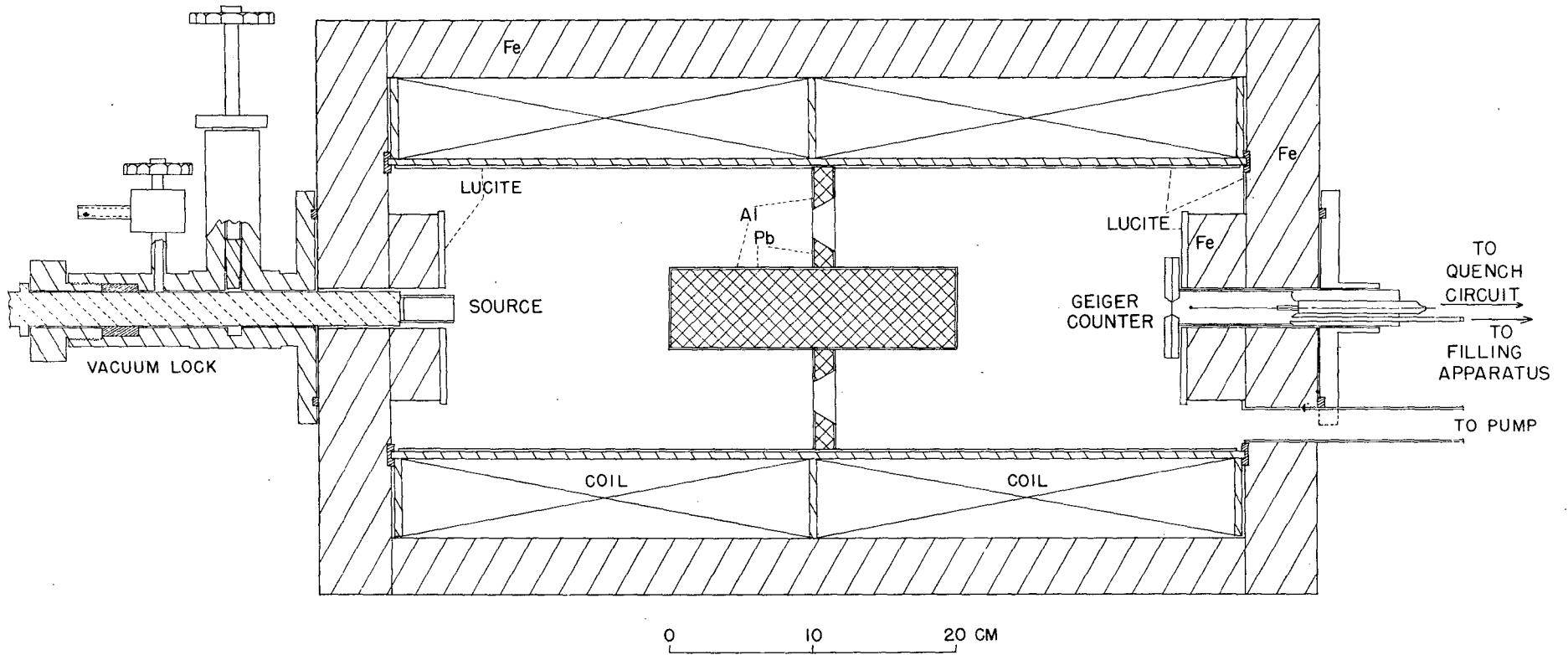
The magnetic lens beta-ray spectrometer described in this paper is similar to that described by Siegbahn¹⁵ where, in order to reduce spherical aberration, the magnetic flux density is altered from the simple longitudinal form to a form where the flux density is thirty percent stronger at the two foci than at a point half way between. With this field form a much greater transmission factor for the same resolving power can be realized.

The magnet consists of an iron tube sixty centimeters in length by forty centimeters in diameter made of two inch square iron bars spaced uniformly around the circumference (see Figure 1). Cylindrical pole pieces four centimeters deep and thirteen centimeters in diameter are affixed to iron end pieces five centimeters thick which are mounted on wheels to render them easily moveable. Cylindrical holes 2.3 centimeters in diameter through the axis of both pole faces are provided for the Geiger tube and the radioactive source.

The coil consists of two solenoids thirty centimeters in length with inside and outside diameters of twenty and thirty centimeters respectively. Each coil is wound with 3600 turns of number twelve enameled copper wire. The resistance of each coil is 17.2 ohms. The coils are arranged so that they may be used in series or in parallel.

The vacuum chamber is composed of the coil form, which is a brass tube twenty centimeters in diameter, and the iron end pieces which butt up against the brass tube through rubber gaskets forming a vacuum tight seal. The entire surface of the vacuum chamber is covered with a layer of polystyrene to reduce electron scattering from the walls.

A Geiger tube of the end window type with a brass cathode six



SCHEMATIC DIAGRAM OF SPECTROMETER

FIG. 1

centimeters in length by two and a half centimeters in diameter is placed before the hole in one of the pole faces so that its end window projects one centimeter in front of the pole face. The end window which is 0.8 centimeter in diameter is usually composed of 0.4 mg/cm² nylon sheet held in place by a clamping ring and sealed with gaskets of dental dam. The Geiger tube is connected by a metal tube to an evacuation and filling apparatus. This apparatus allows the Geiger tube and the vacuum chamber to be evacuated at the same time so that no pressure differential will exist across the thin nylon window. The filling apparatus consists of a number of reservoirs of argon, ethylene, and alcohol together with a mixing chamber and attached manometer so that any desired mixture (usually about eight centimeters of argon and one of ethylene) may be introduced into the Geiger counter. Ethylene is used rather than alcohol when nylon windows are used because of the solubility of nylon in alcohol.

One centimeter before the other pole face the radioactive source is placed. The source is deposited on a thin film of nylon or Formvar varnish supported on the end of a polystyrene tube (see Figure 2). This tube is fixed to a one inch diameter metal rod so that the sample can be introduced into the evacuated region through a vacuum lock consisting of a chevron seal and a gate valve. This is necessary to facilitate the rapid changing of samples without opening the vacuum chamber. The window of the Geiger tube will not tolerate atmospheric pressure.

The shutter and slit system is placed in the center of the spectrograph between the source and the Geiger tube (see Figure 1). The slit is circular with inner and outer radii of five and seven centimeters

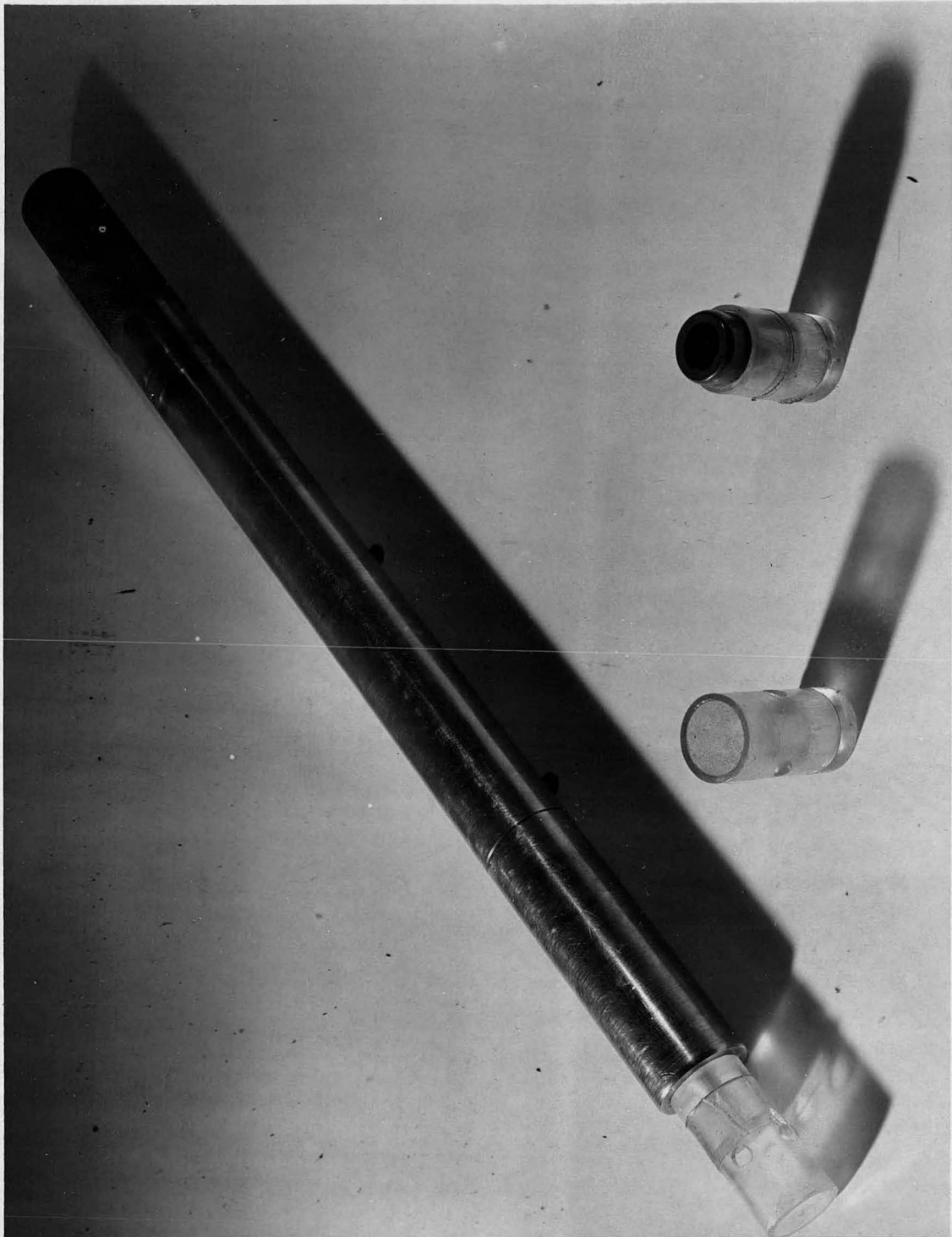


FIG. 2

corresponding to a transmission factor of two percent and a resolving power of about five percent. The resolving power is based on the percentage width at half maximum of the $H\beta$ value of a sharp conversion line. A disc made of aluminum can be introduced so that the inner half of the slit is blocked or covered up. The transmission factor is reduced to about one percent while the resolving power is increased to about three and one-half percent. A cylinder of solid lead twenty centimeters long is placed axially between the source and the Geiger tube to prevent direct gamma-radiation from reaching the counter.

The main vacuum chamber is evacuated by a six inch diffusion pump backed by a "Megavac" mechanical pump. The pressure inside the vacuum chamber is measured with a thermocouple gauge.

The coils of the spectrometer are cooled by forced air passing between the surfaces of the coil and the iron shell.

The power for the coils of the spectrometer comes from a five KVA d.c. generator. Current regulation is accomplished by controlling the voltage across the generator field. This is done to better than one part in a thousand by the following method. The current passing through the spectrometer coil also passes through an adjustable resistance in series with the coil. The voltage across this resistance is compared to a reference voltage consisting of a number of dry cells and the difference between these two voltages is amplified in a four stage cascaded d.c. amplifier having a gain of about 1600 in voltage. As long as the difference between the two input voltages is zero the output of the amplifier is zero, but when there is a slight deviation, the output of the amplifier immediately adjusts a grid controlled rectifier supply which supplies the power for the d.c. field of the

generator so that the coil current returns to the proper value. Course and fine adjustments of the coil current are made by varying the series resistance and the reference voltage. The coil current is measured by means of a standard resistance of 0.2 ohm and a potentiometer which compares the voltage across the standard resistance to that of a standard cell.

With this lens no departure from linearity between the coil current and the focused H_p has been established either by measuring the H_p values of known conversion lines or by direct measurement of the field. At extremely low values of H_p a deviation is present if care has not been taken to demagnetize the instrument, since any residual magnetism in the iron will have a large influence here. Therefore it is customary to demagnetize at the beginning of every run and to proceed only in the direction of increasing current when in the region of low energy. A curve of measured relative flux density as a function of the coil current is shown in Figure 3.

The Geiger tube is connected to a quenching circuit and a preamplifier of low dead time designed by W. Goldsworthy (see Appendix). It is important to have a low dead time in an application such as this since the range in counting rates encountered will be very broad and the necessary corrections for counting loss due to dead time should be kept as low as possible. The output of the preamplifier goes to a Higginbotham type scaler¹⁹ having a scale of sixty-four and then to a counting register. In addition to the scaler there is a counting rate meter (see Appendix) for preliminary investigations of the essential features of the beta spectrum.

When beta-gamma coincidences are to be measured a special source holder must be used. This holder serves as a scintillation counter for

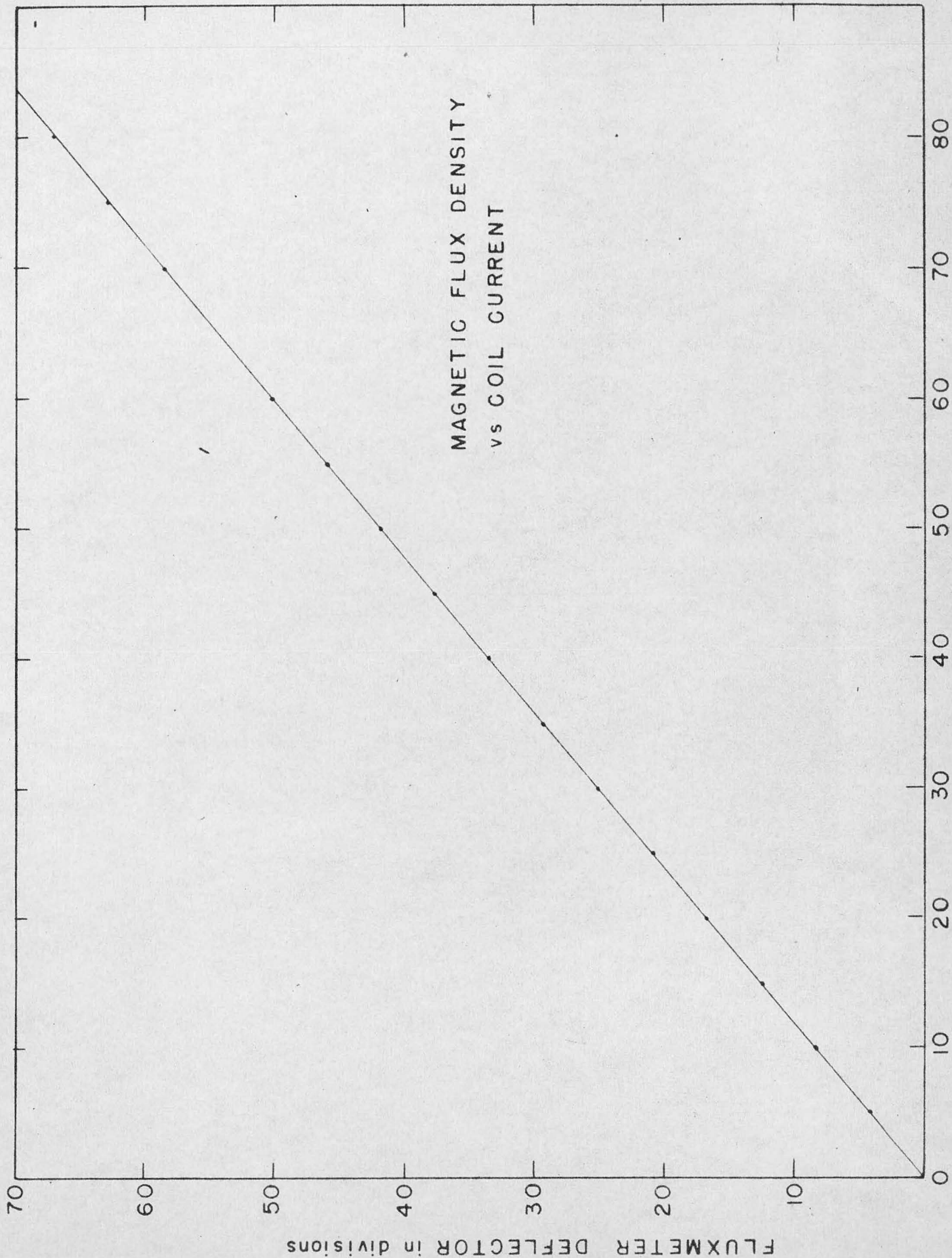


FIG. 3

14535

the gamma radiation from the sample. The outer dimensions of the source holder are similar to the one used before except that the metal rod which is used to introduce the sample into the evacuated region is hollow and closed at the sample end with a beryllium copper foil which maintains the vacuum and serves as an absorber for the beta radiation from the source. Directly behind this absorber is an anthracene crystal mounted on a length of polished lucite rod which acts as a light pipe leading to the photomultiplier tube outside the magnetic field of the spectrometer. The photomultiplier tube is in a container surrounded by dry ice to keep the noise pulses to a minimum.

The pulses from the photomultiplier tube go through an inverter and preamplifier stage with a gain of about two into a wide band pulse amplifier consisting of two three-tube feed back loops having a gain of about twenty-five. The output of this amplifier goes to one channel of a coincidence circuit. In each channel of the coincidence circuit is a blocking oscillator which will give a square output pulse of 0.2 microsecond width; the outputs of these blocking oscillators go into a conventional Rossi coincidence stage. The other input channel comes from the preamplifier of the Geiger counter. The resolving time was made to be 0.2 microsecond since the firing time of the Geiger counter is uncertain to the order of 0.1 microsecond. The output of the Rossi stage goes into a scaler with a scale of four and then to a counting register which gives the coincidence counting rate. A second scaler of the Higginbotham type is provided to observe the counting rate of the scintillation or gamma counter. This system can be made to count beta-beta coincidences with one part of the beta spectrum spectrally resolved if the absorber between the source and crystal is made thin

enough to transmit beta radiation and the anthracene crystal is made very thin so as to have poor efficiency for counting gamma radiation and high efficiency for counting beta radiation.

A multiple source holder has been used in conjunction with the spectrometer. It consists of ten sources mounted on a wheel spaced evenly about a given radius (see Figure 4). This wheel can be rotated from the outside of the spectrograph where an indicator tells which of the ten samples is in the proper position. In front of the wheel there is a lead baffle covered with polystyrene with an opening at one point so that only the radiation from the one desired sample can be transmitted through the spectrograph. Such a multiple source holder has been used by G. M. Temmer²⁰ to measure excitation functions.

All helical type spectrometers transmit both electrons and positrons at the same time, the two different particles spiralling in the opposite sense. Occasionally it is necessary to make an experimental identification of the type of particle and for this purpose a baffle is provided (see Figure 5). Vanes are placed in front of the slit in the spectrograph such that only those particles spiralling in the correct sense are transmitted. A reversal of the magnetic field allows the particles of the opposite sign to get through and hence the two types can be easily identified. The spectrograph is normally operated with this baffle removed since the scattering that it introduces lowers the resolution to about eight percent.

A general block diagram and a photograph of the apparatus are shown in Figures 6 and 7.

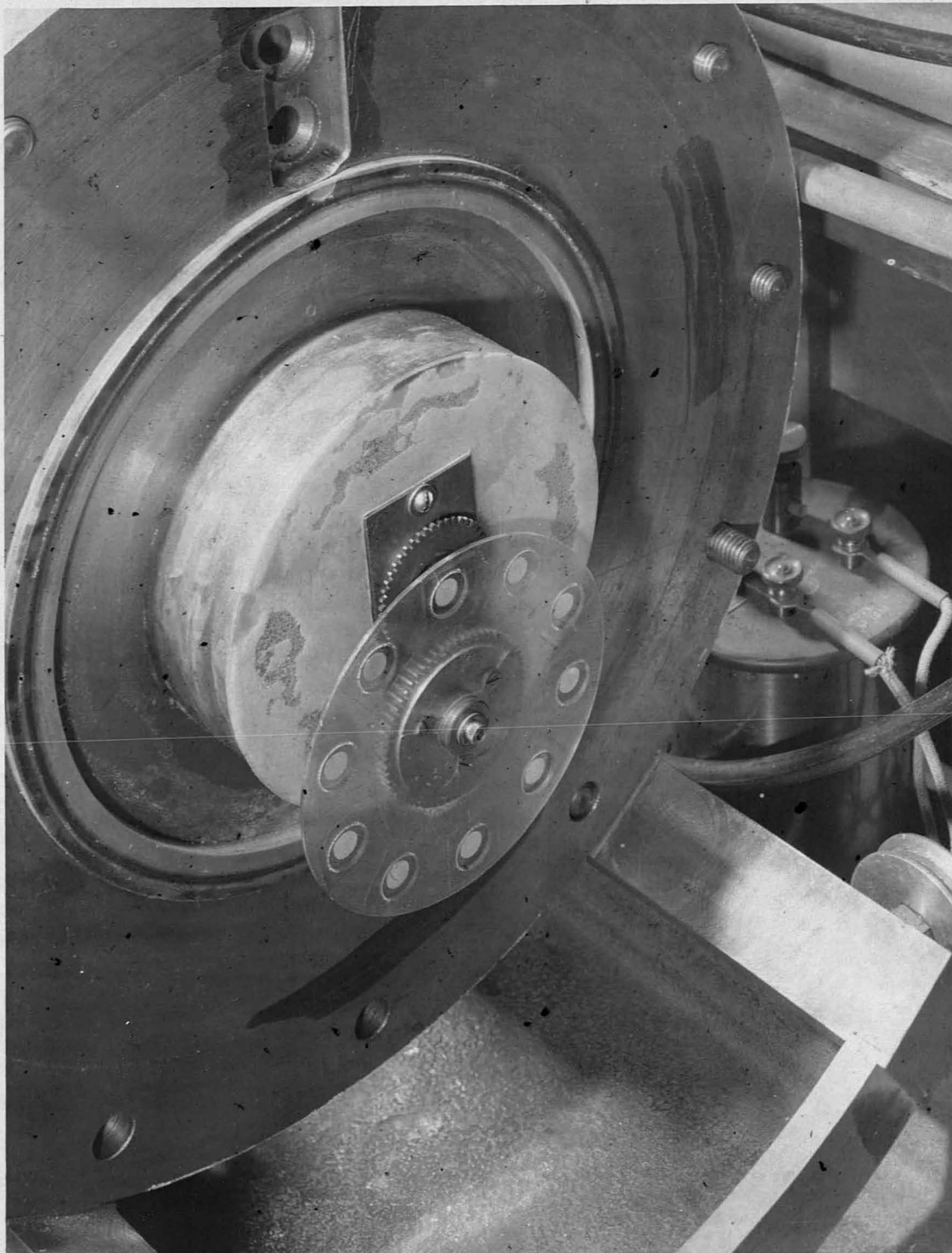


FIG. 4

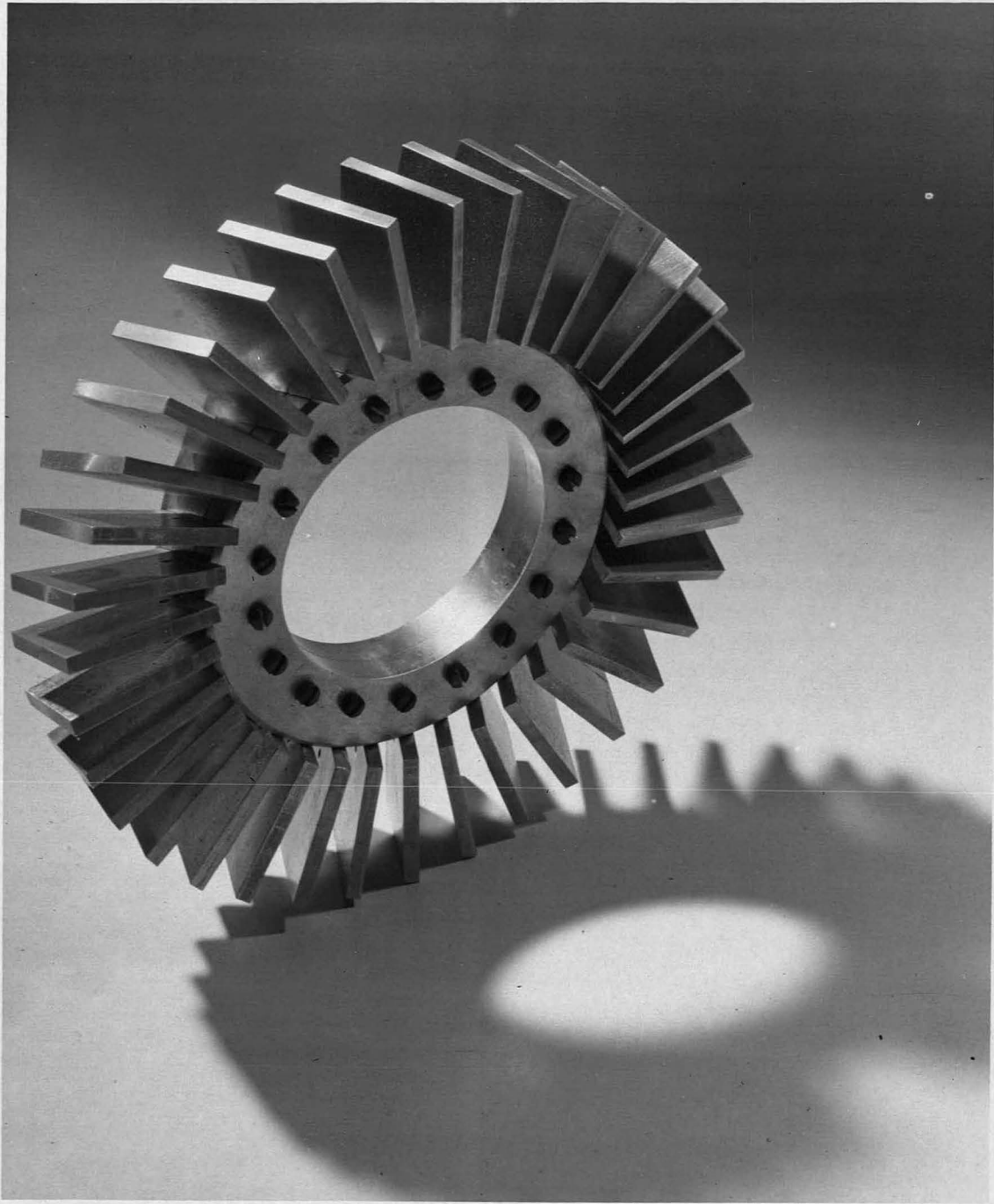
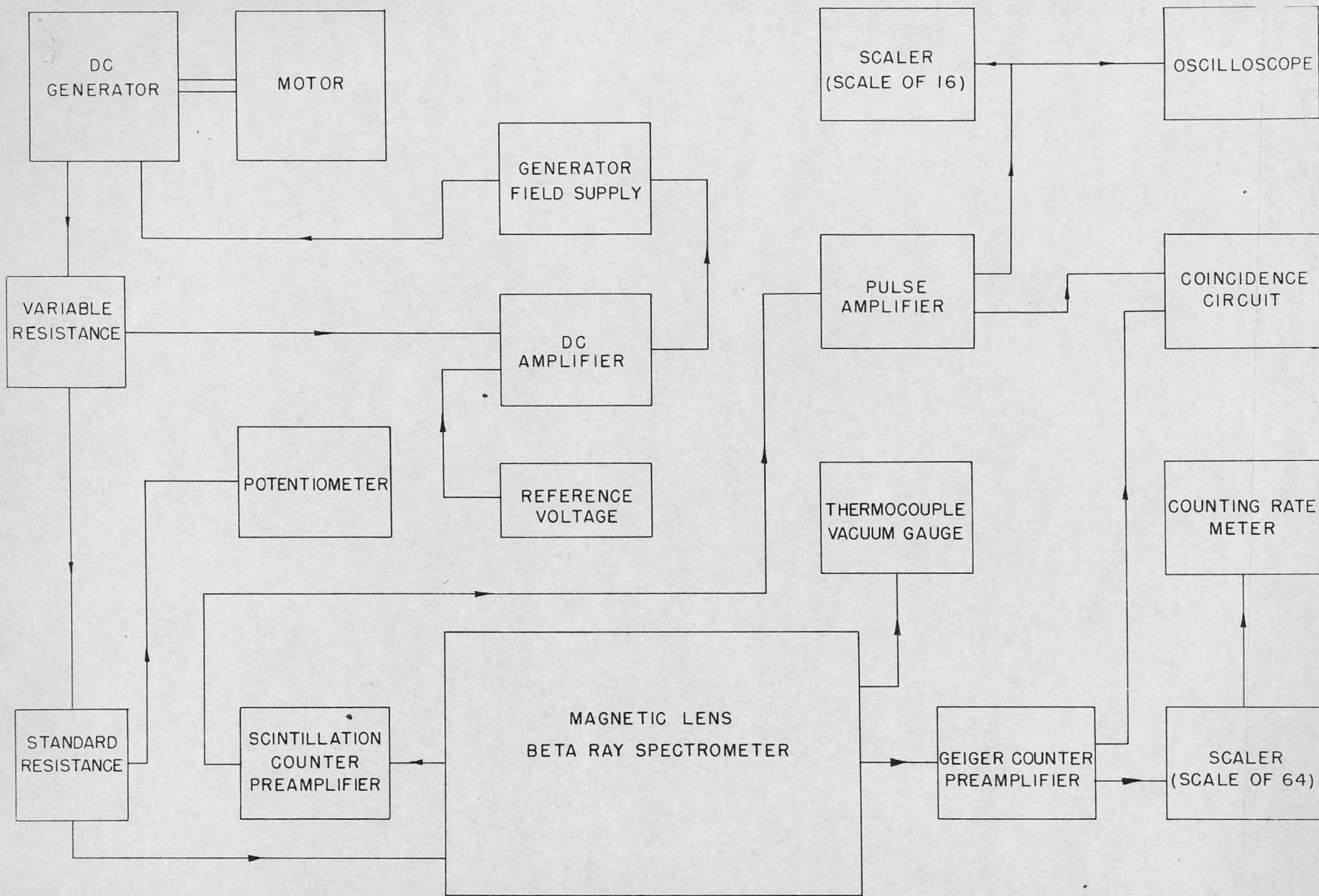


FIG. 5



BLOCK DIAGRAM OF ELECTRICAL COMPONENTS

FIG. 6

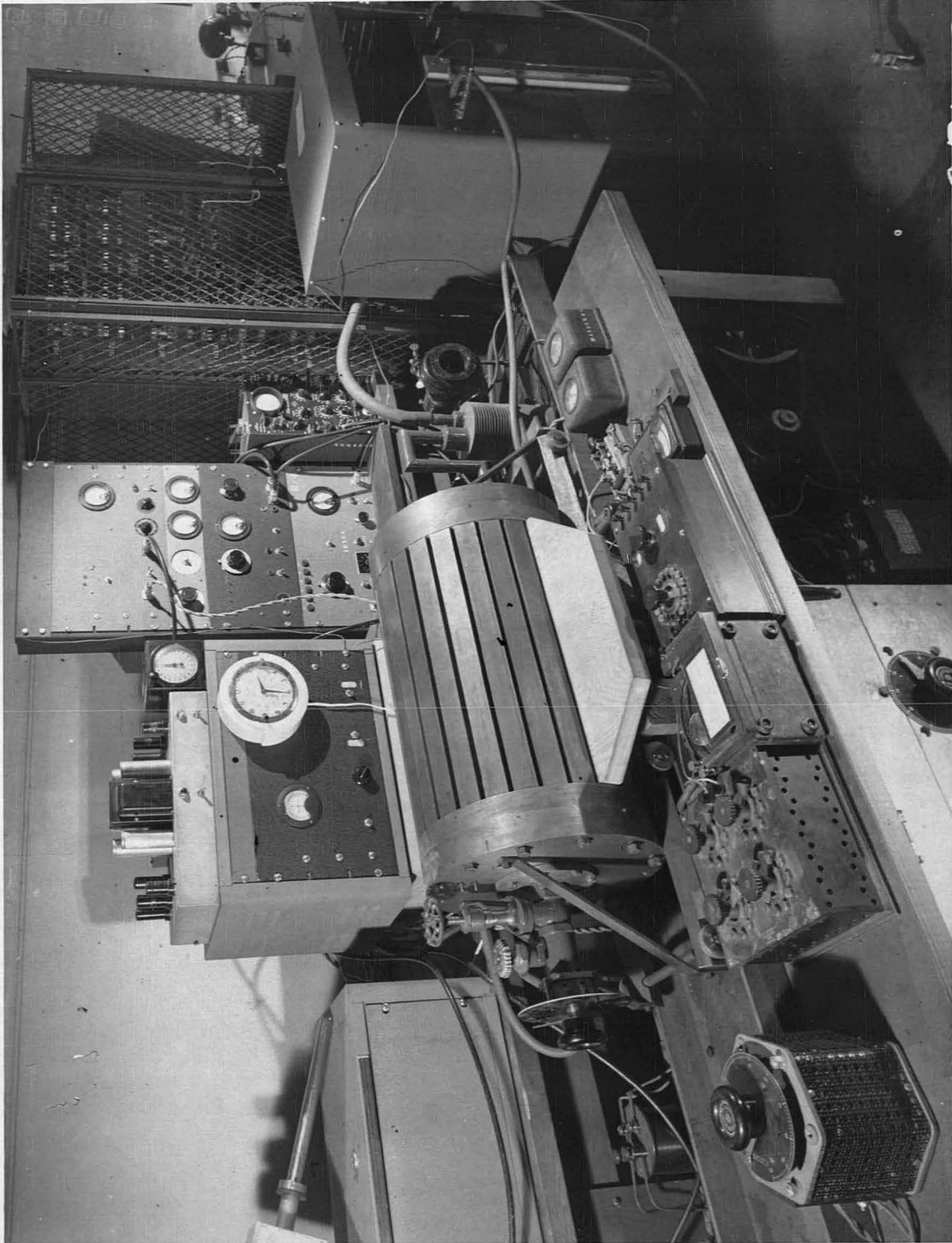


FIG. 7

Experimental Results

Tin 117

The 14 day tin activity was first found by Lindner²¹ in connection with the investigation of spallation products from the high energy deuteron bombardment of antimony. He observed both conversion electrons and gamma radiation and assigned the activity to Sn¹¹⁹ on the basis of cross section arguments. Recently Mihelich and Hill²² have assigned this activity to Sn¹¹⁷ by irradiating enriched isotopes of tin with slow neutrons.

A sample was prepared by bombarding a thick target of antimony with 100 Mev deuterons. Chemical procedures similar to those of Lindner were used to separate the tin. It was necessary to use a large amount of tin carrier (5 mg) as the tin is separated from the antimony and purified by selective precipitation as sulfides. A source was prepared by mounting the separated tin on a Formvar film backing so that the total thickness was about one mg/cm². The observed conversion electron spectrum is shown in Figure 8. Two conversion peaks are present at 124.5 Kev and 150.1 Kev corresponding to the conversion of a gamma-ray of 0.154 ± 0.003 Mev; this value is slightly smaller than the value of 0.159 Mev obtained in the preliminary investigation of Mihelich and Hill²². From the value of the lifetime of 14 days and the energy of 0.154 Mev the transition would correspond to a change in angular momentum of 5 according to the experimental and theoretical classifications of Axel and Dancoff¹¹. The experimental value of the ratio of the K and L conversion electrons is 2.2 which might be subject to a small error because of source thickness. With the value of $\ell = 5$ the theory of Hebb and Nelson¹³ gives 0.95 as the theoretical K/L ratio for electric transitions and 2.85 for

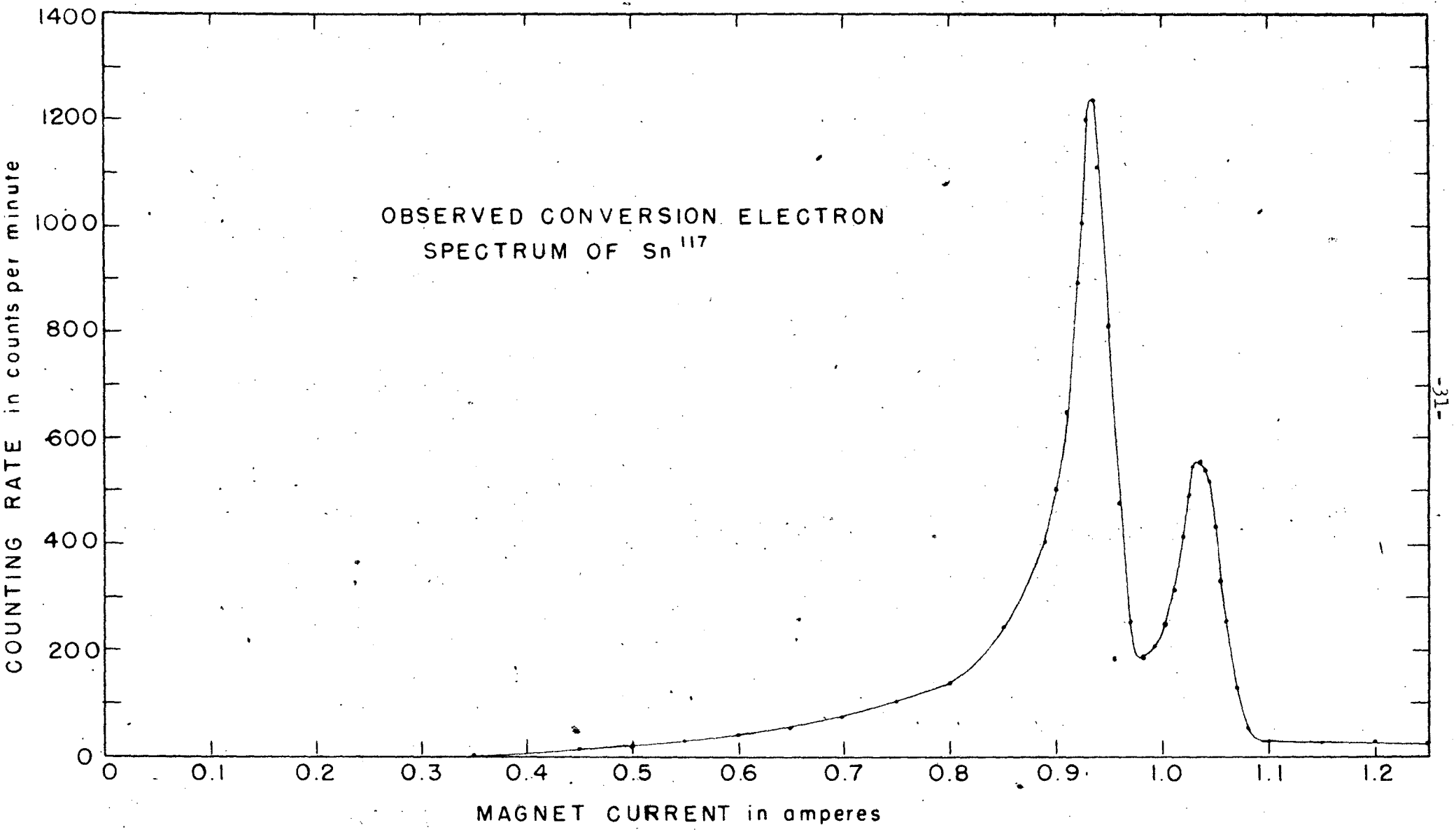


FIG. 8

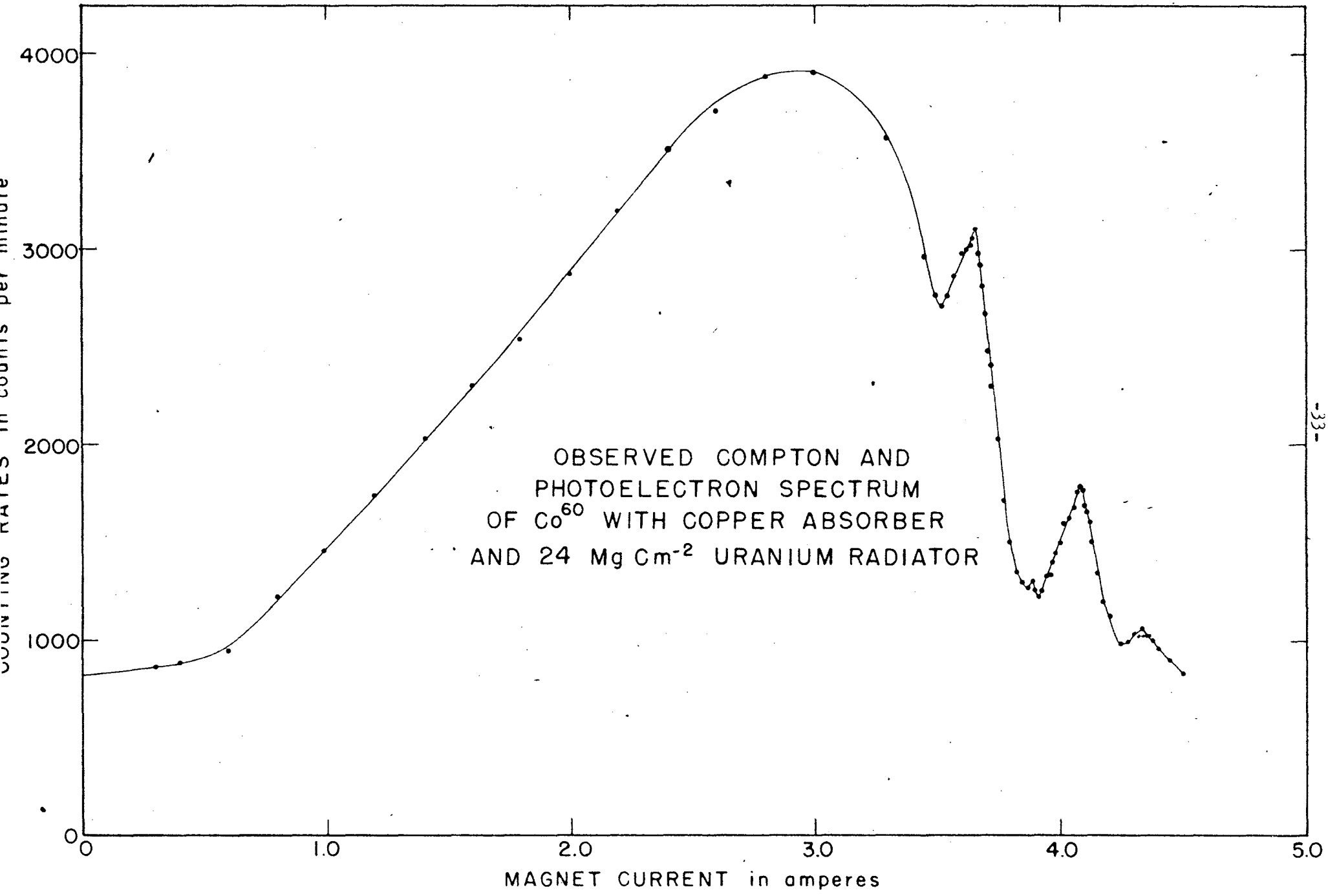
magnetic transitions. For magnetic transitions with $l = 4$ the K/L ratio is 3.85. Therefore in order to account for the K/L ratio a mixture of 2^5 pole electric and 2^4 pole magnetic radiation must be postulated.

The above energy values are based on the calibration that one ampere through the coils of the spectrometer focuses an electron with $H\rho$ of 1350 ± 10 gauss centimeters. This calibration was made for seven different values of $H\rho$. Four points were obtained from the K and L photoconversion lines in 24 mg/cm^2 of uranium by the 1.3316 ± 0.0010 Mev and 1.1715 ± 0.0010 Mev gamma-rays measured absolutely by DuMond and co-workers²³. Another two points were obtained from the K and L photoconversion lines in 10 mg/cm^2 of gold of the 0.51079 ± 0.00006 Mev positron annihilation radiation also measured by DuMond²⁴. A final point is from the 1385 $H\rho$ "F" conversion line from thorium B. A typical photoconversion spectrum of Co^{60} used for calibration purposes is shown in Figure 9.

Copper 62 - Zinc 62

The positron spectrum of the ten minute Cu^{62} was first observed by Crittenden²⁵ in a cloud chamber. More recently Becker²⁶ studied the spectrum in a beta spectrometer using sources of copper foil which had been irradiated with 22 Mev x-rays from the Illinois betatron. His method of observation required the use of rather thick sources (11 mg/cm^2) since no chemical separation could be made. Also because of the short lifetime of Cu^{62} a number of samples had to be used making it necessary to normalize each observed interval with the preceding one.

A more convenient method of observing the Cu^{62} spectrum would be to use its parent Zn^{62} as a source. Zn^{62} was reported by Miller²⁷



OBSERVED COMPTON AND
PHOTOELECTRON SPECTRUM
OF Co^{60} WITH COPPER ABSORBER
AND 24 Mg Cm^{-2} URANIUM RADIATOR

FIG. 9

-33-

as a K-capture activity with the half-life of 9.5 hours, thus the Cu^{62} formed by the decay of Zn^{62} would appear to decay with this longer lifetime. A sample of Zn^{62} was prepared by bombarding a thick copper target with 100 Mev deuterons in the 184-inch cyclotron. The reaction is $\text{Cu}^{63}(\text{d},\text{n})\text{Zn}^{62}$. The Zn^{62} was separated by first electroplating out the majority of the copper and then performing a chemical separation on the remainder. Only about 100 micrograms of carrier was added so that a thin source of about 0.1 mg/cm^2 thickness on a backing of Formvar film was prepared. The beta spectrum is shown in Figure 10. There are three features in this spectrum, a high energy positron component arising from the decay of Cu^{62} , a lower energy positron component from the decay of Zn^{62} , and two conversion peaks corresponding to the K and L conversion lines of a 41.8 ± 0.8 Kev gamma-ray following the decay of Zn^{62} since the energy separation of the K and L lines is just equal to the difference between the K and L binding energies in copper. At this low energy the absorption of the 0.4 mg/cm^2 nylon window of the Geiger counter begins to have some effect so that the K conversion peak is probably absorbed slightly more than the L conversion peak. Hence the observed ratio of the K and L conversion electrons would set a lower limit on the actual ratio. This ratio is approximately 6.4 and would correspond to either an electric or magnetic dipole transition. A Fermi plot of the positron spectrum is shown in Figure 11. The upper limit of the Cu^{62} positron spectrum obtained from this plot is 2.92 ± 0.02 Mev and is about two percent higher than the value of Becker²⁶. Subtraction of the extrapolated straight line Fermi plot for Cu^{62} from the total spectrum gives the Fermi plot for Zn^{62} shown in Figure 12. The upper energy limit for Zn^{62} is 0.685 ± 0.010 Mev. The curvature in this Fermi plot can be

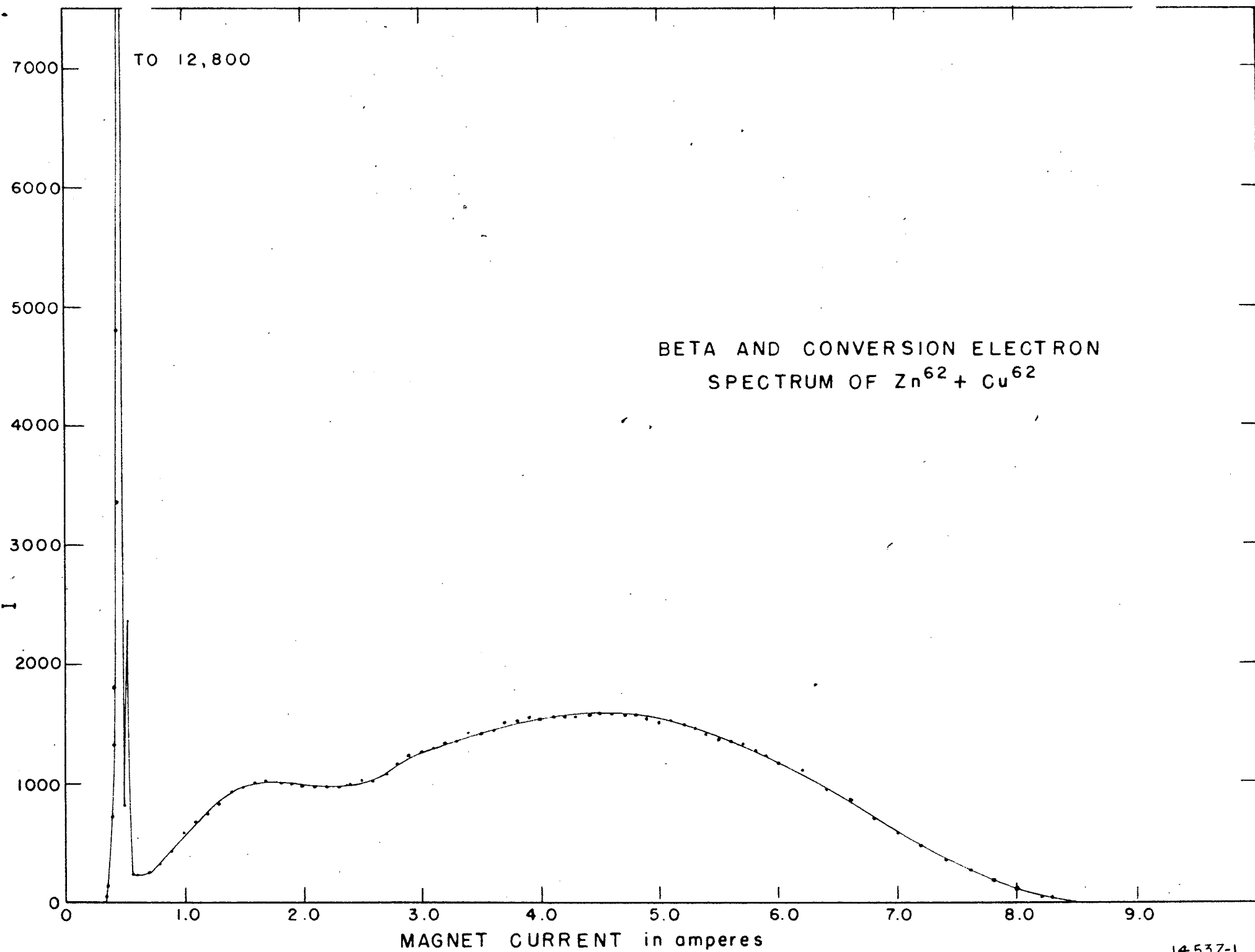


FIG. 10

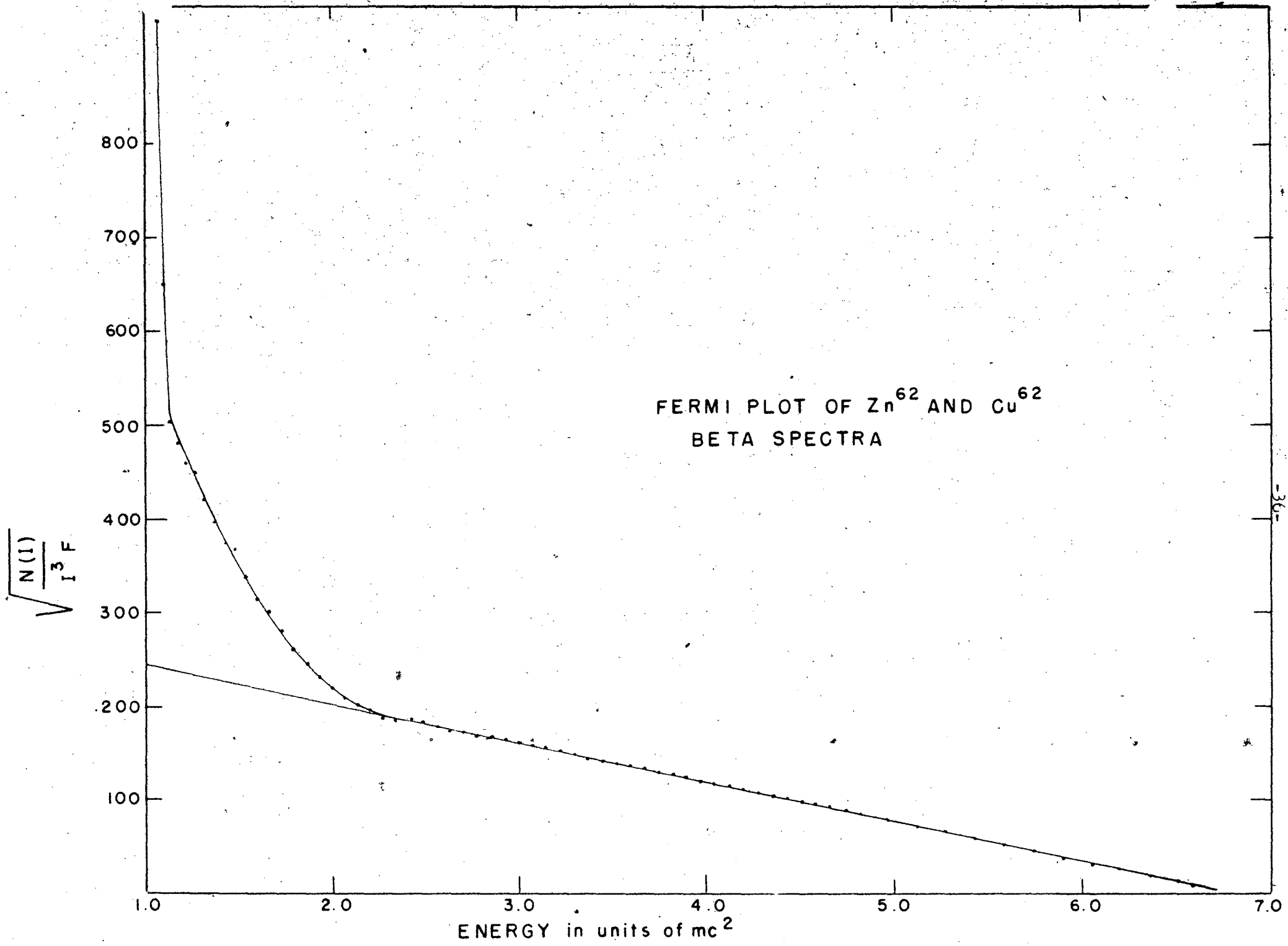
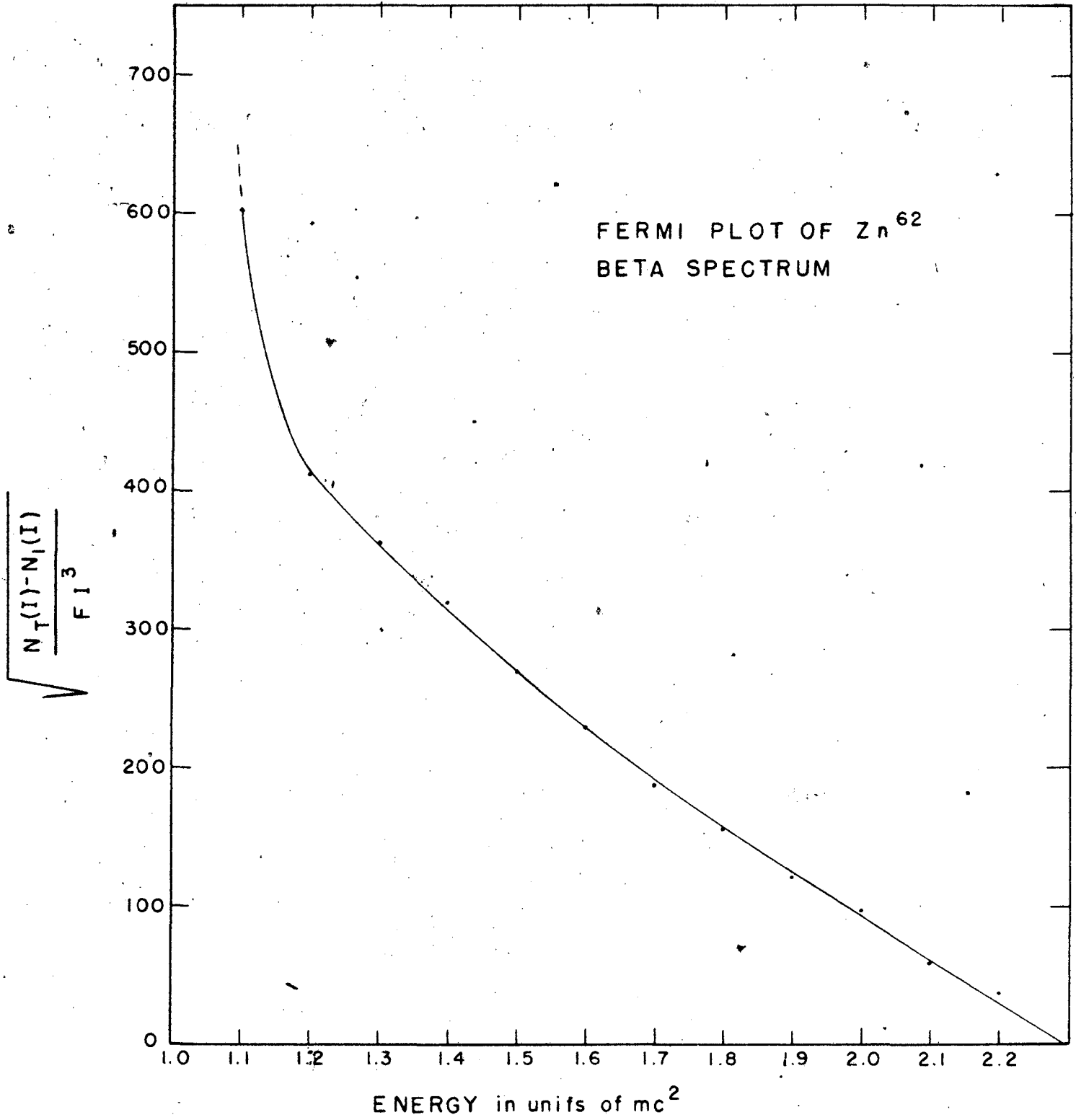


FIG. II



· FIG. 12

attributed to a small amount of back scattering from the much more intense Cu^{62} spectrum. The half-life of Zn^{62} is 9.33 hours as indicated by Figure 13. Comparison of the number of positrons in both the Zn^{62} and the Cu^{62} spectra indicates that Zn^{62} decays about ten percent of the time by positron emission and the remainder by K-capture. According to the Fermi theory of beta decay positrons should be emitted twenty-five percent of the time. This sort of discrepancy is common because of the very strong energy dependence of the probability for positron emission. Perhaps a slight error in the upper energy determination would account for this difference. The nuclear matrix elements should be the same for both K-capture and positron emission. However, another complication is the lack of knowledge of the branching ratio of the Zn^{62} decay where the decay might take place to two states separated by 41.8 Kev. This would be difficult to determine without experimental knowledge of the conversion coefficient. The Cu^{62} has a $f \tau_{1/2}$ value of 13.4×10^4 and the Zn^{62} has a $f \tau_{1/2}$ value of 5.3×10^4 (taking into account the decay by K-capture and positron emission) which experimentally classifies both spectra as allowed.

Absorption measurements have indicated a maximum energy of 2.5 Mev for the positron spectrum of Cu^{62} . Because of the very wide discrepancy of the values of the upper energy limit obtained from beta spectrometers and from absorption, suspicion was put on the validity of Feather's rule for high energy positrons. Since the Cu^{62} activity is often used as a monitor for hard gamma radiation from synchrotrons and betatrons, it was thought to be profitable to make a careful check to see if absorption techniques could make a good determination of the upper energy limit of the positron spectrum. Absorption curves for both $\text{Zn}^{62} + \text{Cu}^{62}$ and U_3O_8

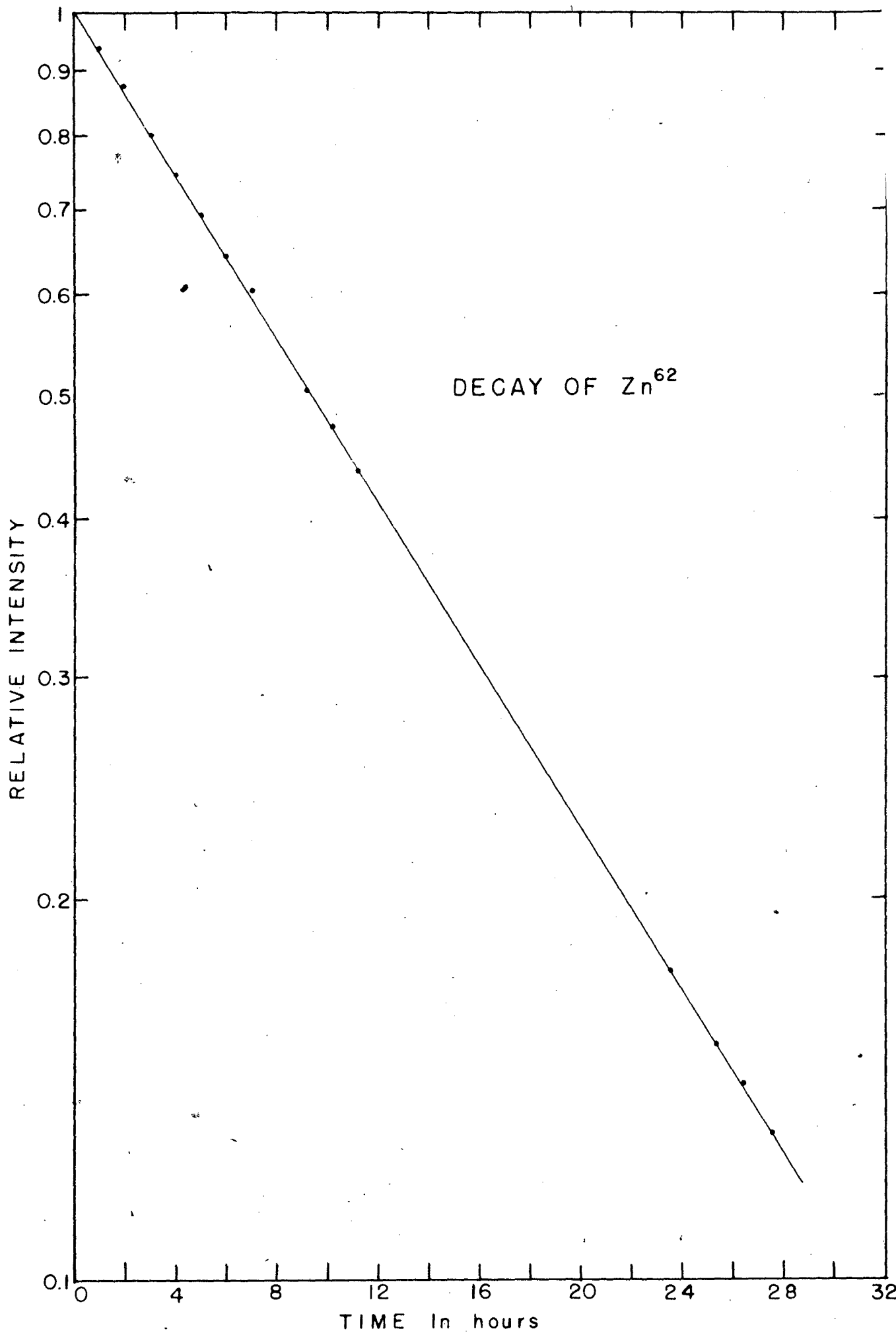


FIG. 13

samples were made exercising great care to keep geometry for both samples the same. Corrections for decay of both sample and background were made since annihilation radiation accounts for part of the background. Absorption curves are shown in Figures 14 and 15, and the Feather analysis is shown in Figures 16 and 17. The value of the upper limit obtained is 3.15 Mev, far higher than other absorption measurements. The only conclusion that can be drawn is that Feather's rule is valid but the experimental method is inherently inaccurate.

Indium 111

The investigation of the 2.7 day K-capture activity of In^{111} was undertaken in conjunction with the other isobaric activities Ag^{111} and Cd^{111} . This activity was first investigated by Lawson and Cork²⁸ who reported conversion lines corresponding to gamma energies of 0.173 and 0.247 Mev. Coincidence measurements made on these two gamma-rays by Bradt²⁹ show that the two gammas are emitted in cascade. The sample of In^{111} was made by a $(\alpha, 2n)$ reaction on silver, and a source was prepared of a few mg/cm^2 thickness including the nylon film backing. The spectrum was taken and is shown in Figure 18. Four conversion peaks are present having energies of 142.2, 164.9, 215.5, and 239.9 Kev. The first two values correspond to energies of K and L conversion lines for a transition of 0.169 ± 0.004 Mev in cadmium. The latter two peaks correspond to a 0.243 ± 0.004 Mev transition in cadmium. Because of the rather high threshold for the reaction it was thought that some positron emission might be present. A search for positrons with the baffle described above proved unsuccessful.

The 0.243 Mev gamma-ray is the same as the one observed in the decay of the Cd^{111} isomer which has an upper state of 48 minutes half-life and which decays with the emission of a highly converted 0.149 Mev gamma-ray.

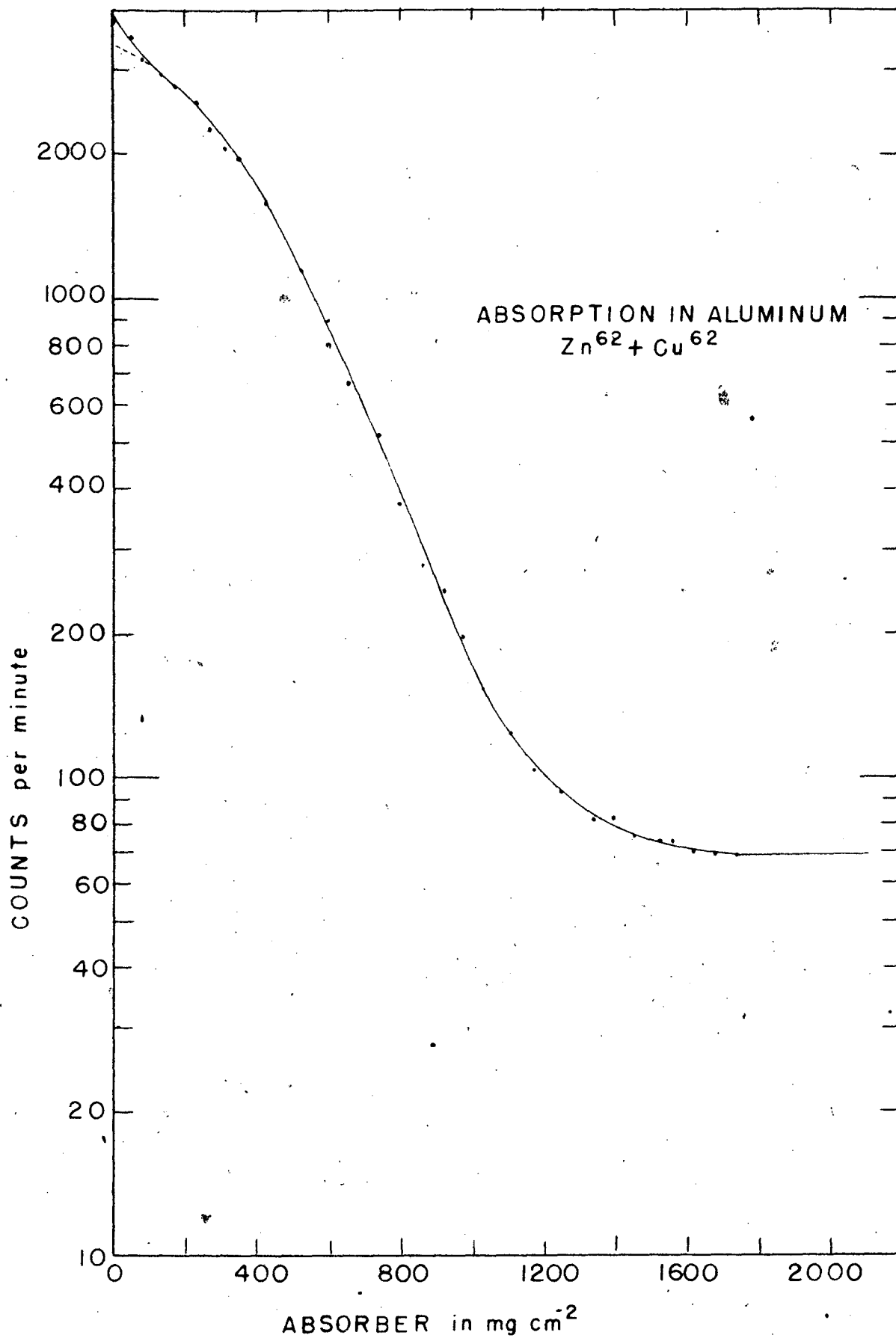


FIG. 14

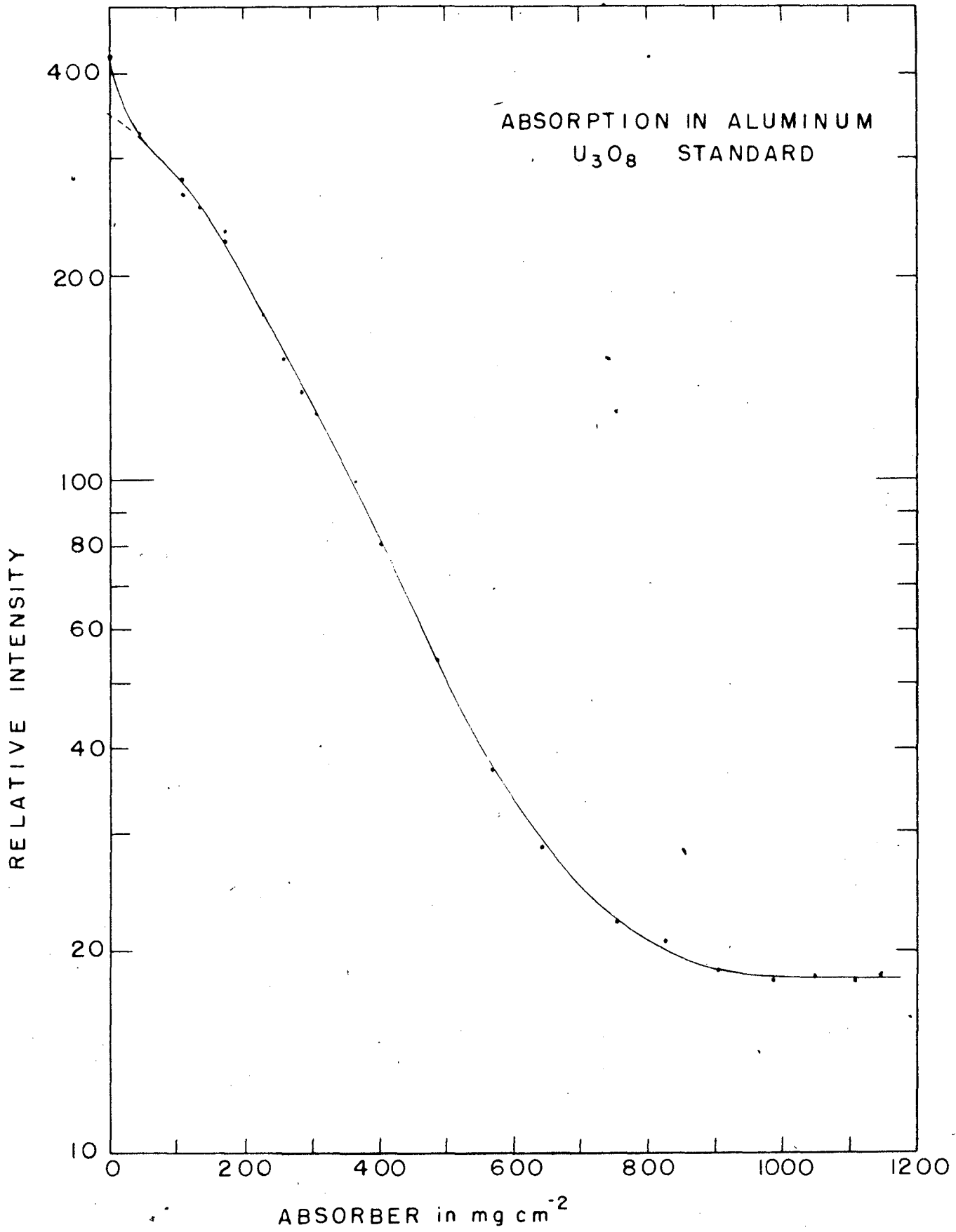


FIG. 15

FEATHER ANALYSIS OF Cu^{62} BETA SPECTRUM

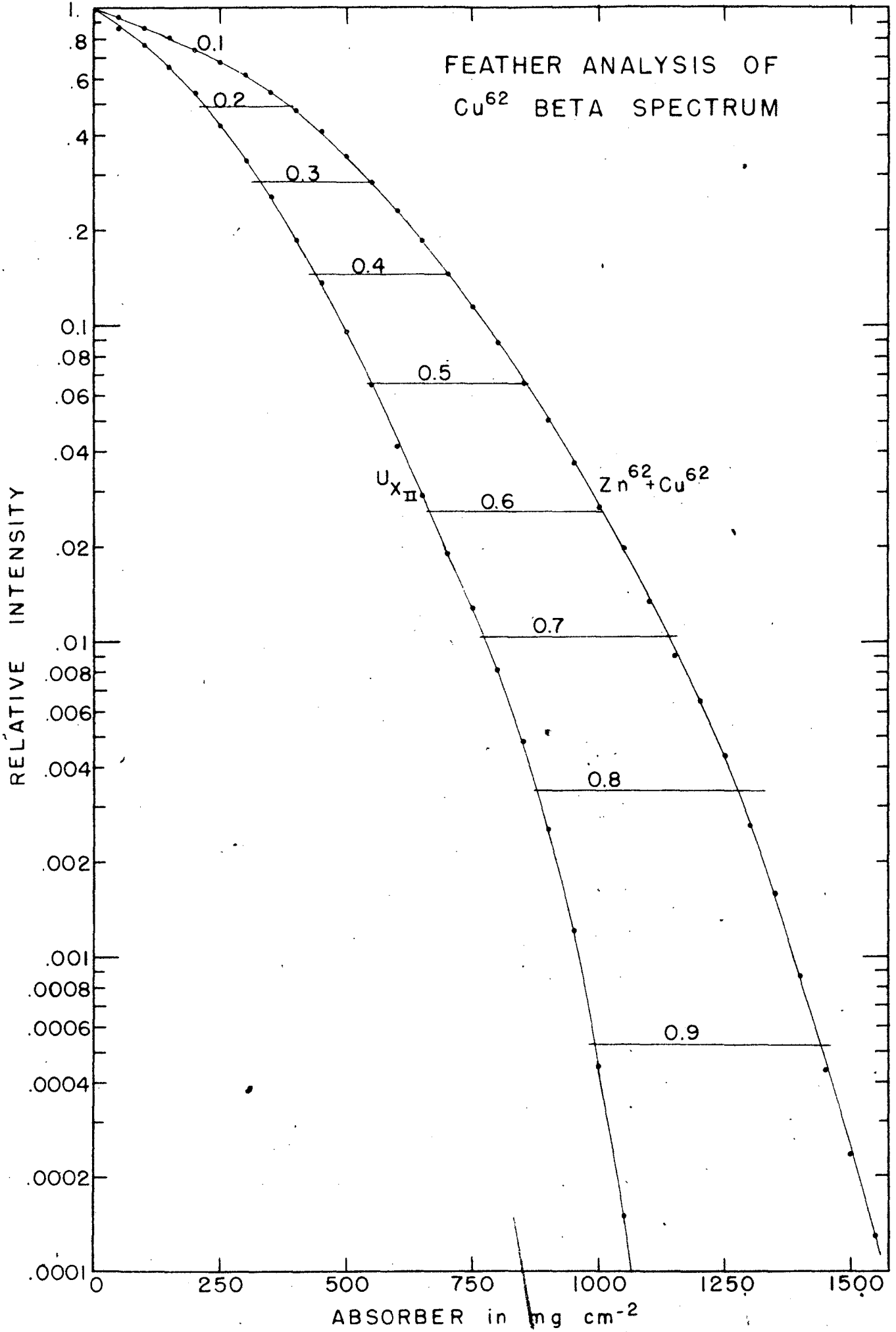


FIG. 16

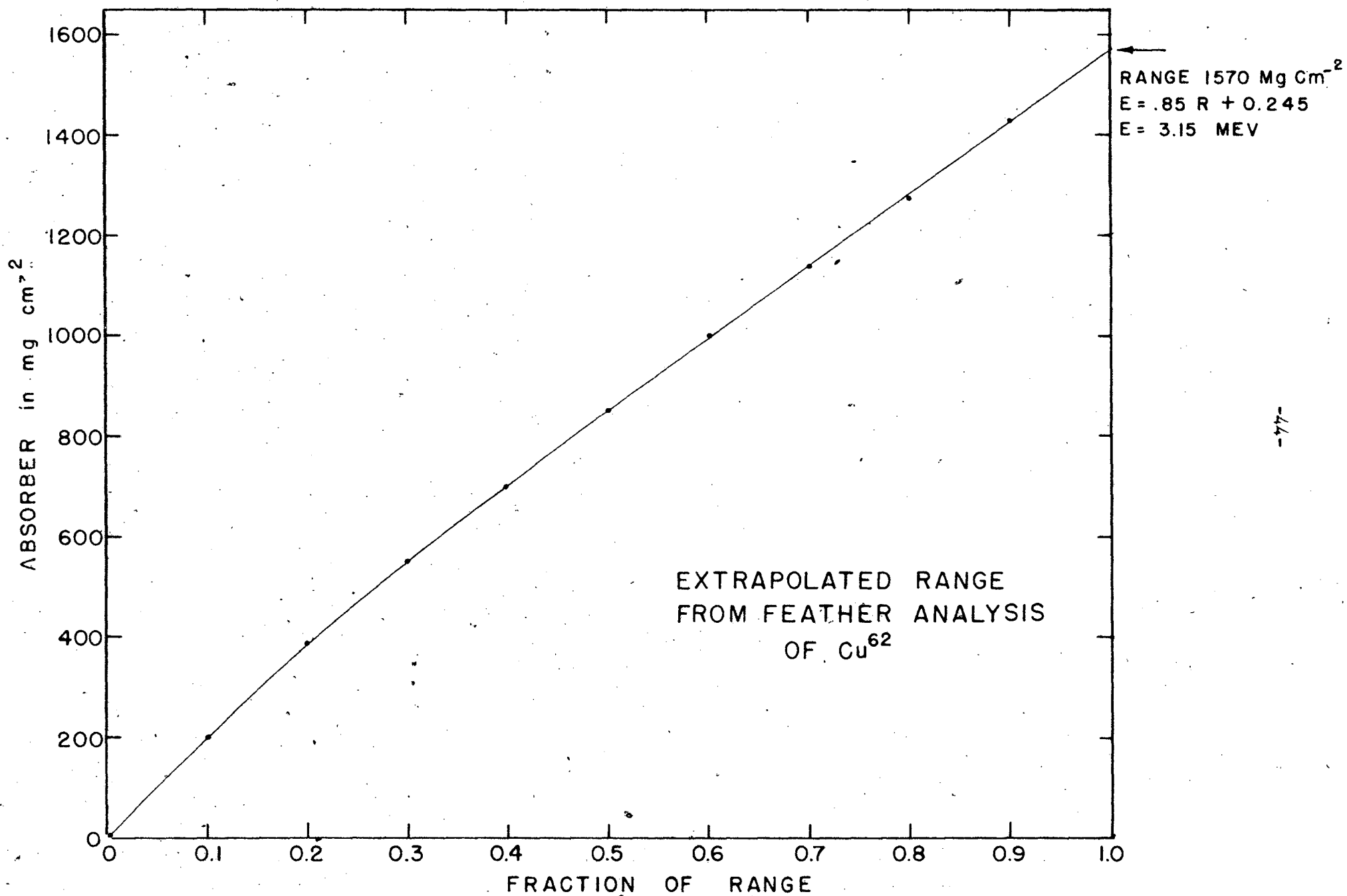


FIG. 17

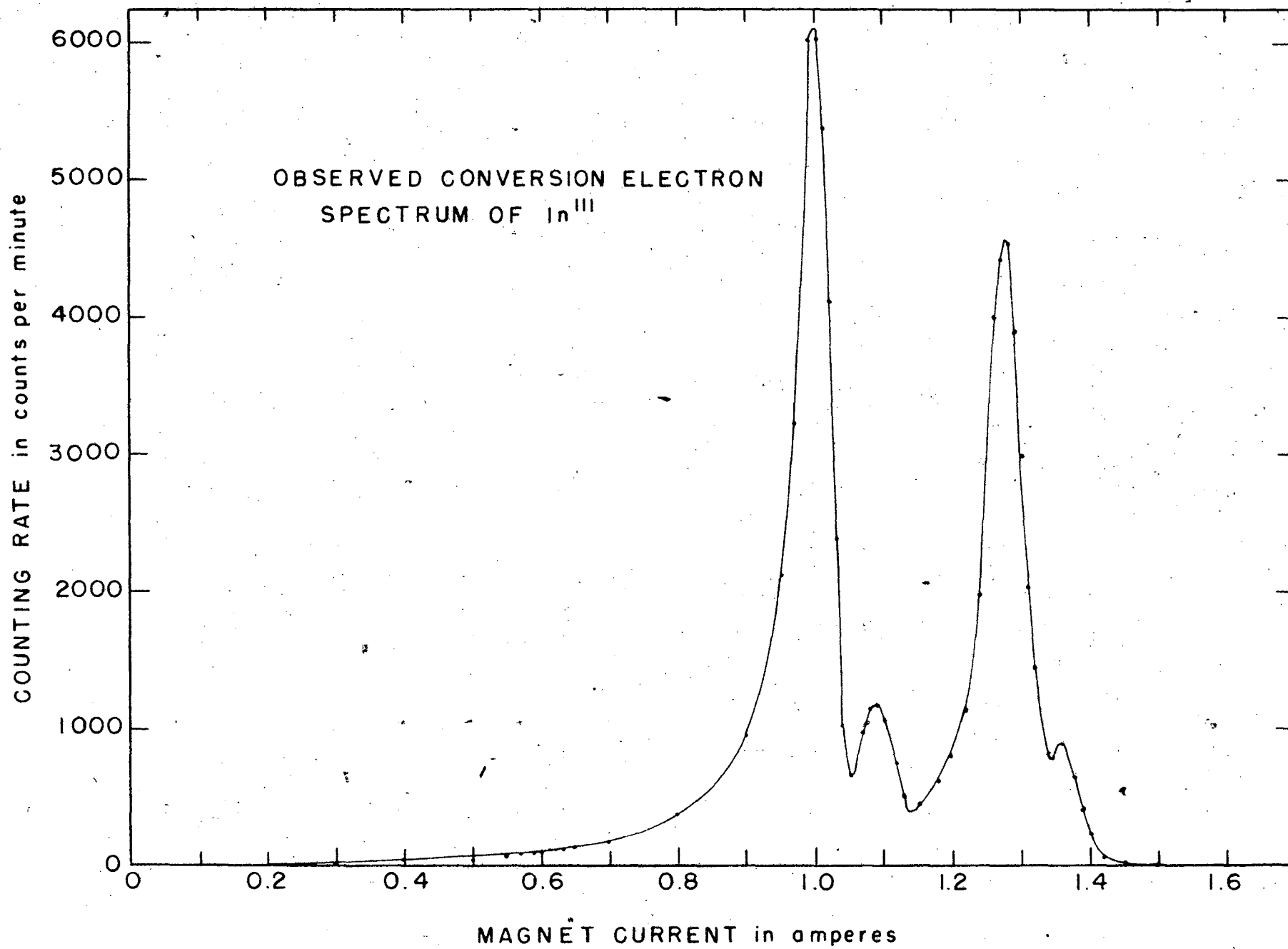


FIG. 18

-46-

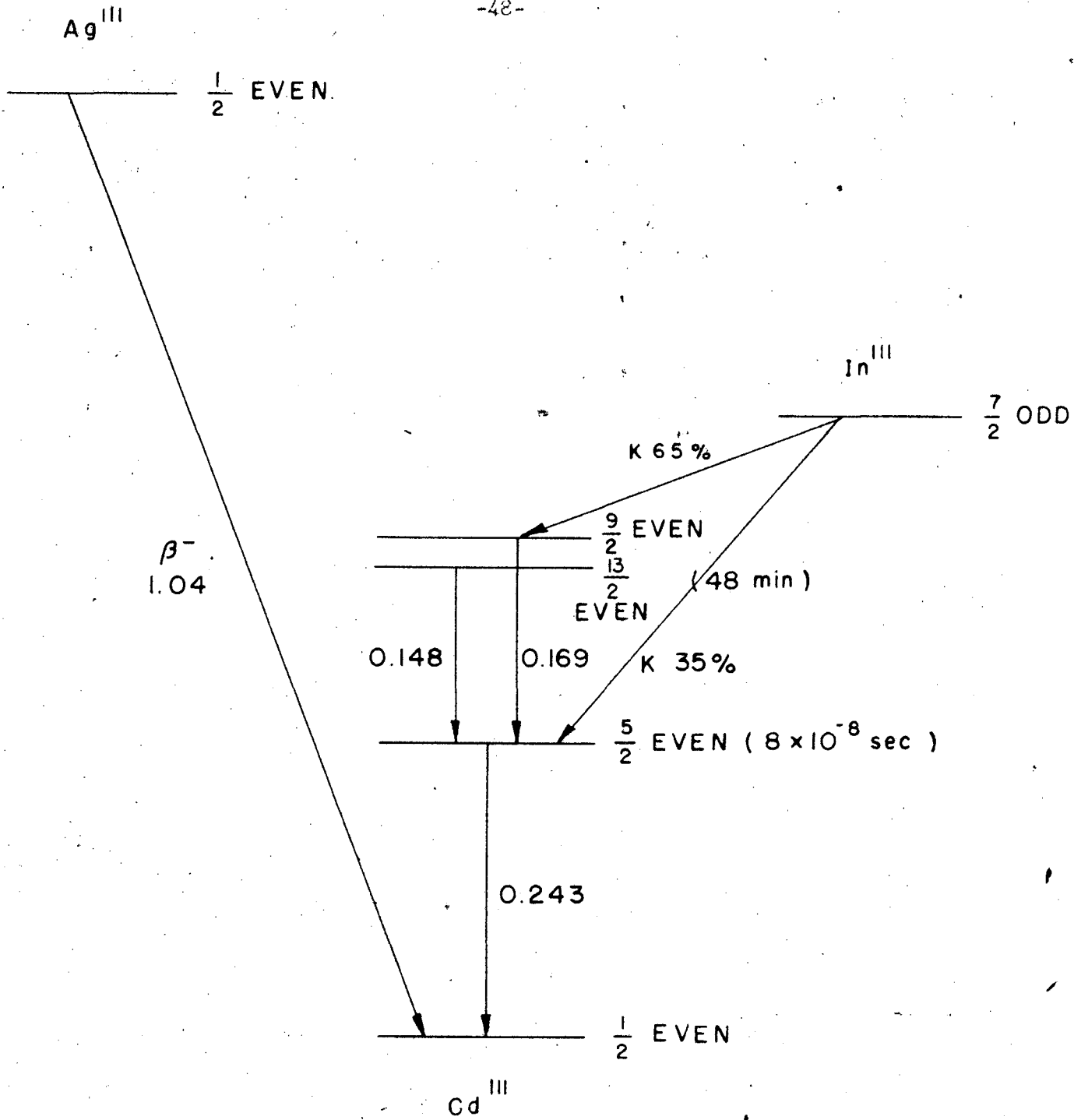
The ratio of the conversion coefficients of these two gamma-rays has been measured by Mr. C. L. McGinnis with the spectrometer described here. He finds the ratio of the number of conversion electrons for the 0.149 and 0.243 Mev gammas to be about 10. With this information and with the knowledge that the two gamma-rays originating from the In^{111} decay are in cascade one should be able to form a decay scheme in which the experimentally observed features would serve as a check on the theoretical conclusions. From the lifetime and the energy of the Cd^{111} isomer one can find that the transition according to the classification of Axel and Dancoff¹¹ involves a change of four units of angular momentum and from the ratio of the K/L conversion electrons the transition is an electric 2^4 pole. The conversion coefficient according to the tables of Rose¹⁴ would then be 7.4. Then the conversion coefficient for the 0.243 Mev gamma-ray is 0.097. The ratio of the number of conversion electrons from the 0.169 Mev transition to the number from the 0.243 Mev transition is 1.7. Again from the tables of Rose if one takes ratios of K conversion coefficients for the two transitions for all possible combinations of multipole orders both electric and magnetic and compares them to the experimentally observed ratio of 1.7, all transitions can be ruled out except where both transitions are both electric quadrupole or magnetic dipole. Deutsch³⁰ has shown that the half-life of the 0.243 Mev state is 8×10^{-6} second, which is not inconsistent with an electric quadrupole transition. These transitions give $\frac{\alpha_{169}^2}{\alpha_{243}^2} = 2.74$ and $\frac{\beta_{169}^1}{\beta_{243}^1} = 2.57$.

All ratios lower than 1.7 can be ruled out as contrary to observed facts; all those much larger would indicate an excessive branching of the In^{111} K-capture decay to the lower state. However, in order to reconcile the disagreement between 1.7 and 2.6-2.7 a branching ratio of about 35 percent

would have to be postulated. Such a decay scheme is shown in Figure 19. It would be consistent to assign the same or one more degree of forbiddenness to the transition to the lower state, as positron radiation does not occur and the transition probability is about the same. As required by being even the parities of all states of Cd^{111} would be the same. The spin of Cd^{111} in the ground state is $1/2$ so the spin of the 0.243 Mev level would have to be $5/2$ and the 0.410 Mev level $9/2$. The spin of the isomeric state would have to be $13/2$ on this basis.

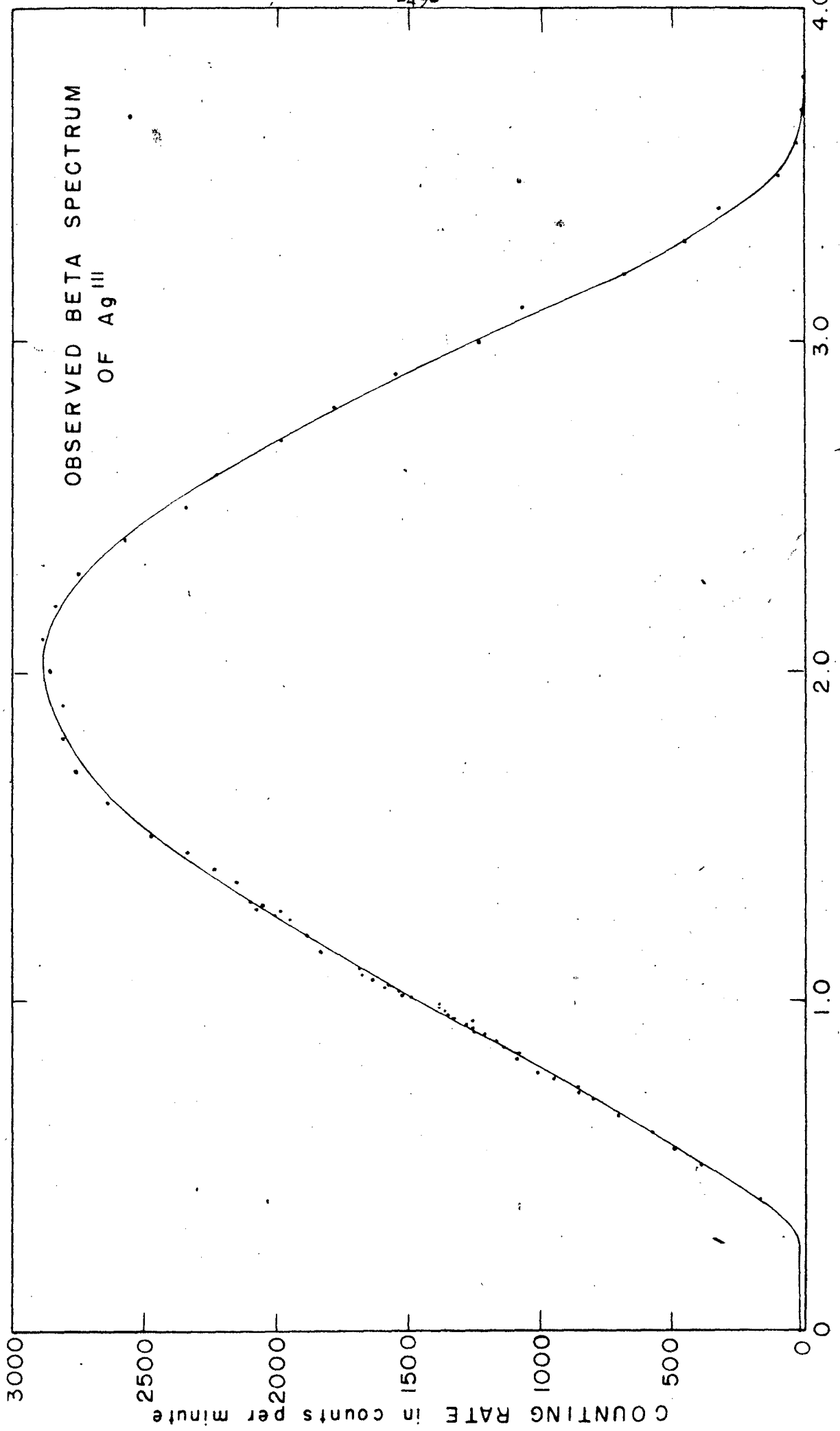
Silver 111

The study of the 7.5 day Ag^{111} was undertaken in connection with the other isobaric activities In^{111} and Cd^{111} in order to correlate the decay scheme shown in Figure 19 in connection with the discussion of In^{111} . Ag^{111} has been studied by a number of investigators^{31,32} who by absorption measurements determined that there was no apparent gamma radiation besides a continuous beta spectrum with upper limit around 1 Mev. In order to confirm this a sample of Ag^{111} prepared by separating silver from palladium bombarded with neutrons was mounted on a nylon film so that the total source thickness was of the order of a few mg/cm^2 . The beta spectrum was examined quite carefully for conversion electrons particularly in the region of the conversion lines of In^{111} . No evidence was found for anything but a simple beta spectrum which is shown in Figure 20. A Fermi plot of this spectrum is shown in Figure 21. The upper energy limit from this plot is 1.04 ± 0.02 Mev. The fact that no gamma transitions are observed requires that any transition to an upper state be at least once more forbidden than the one to the ground state. This requires that the parities be the same for the initial and final states otherwise the degree of forbiddenness would be the same to the



DECAY SCHEME OF Ag¹¹¹, Cd¹¹¹ AND In¹¹¹

FIG. 19



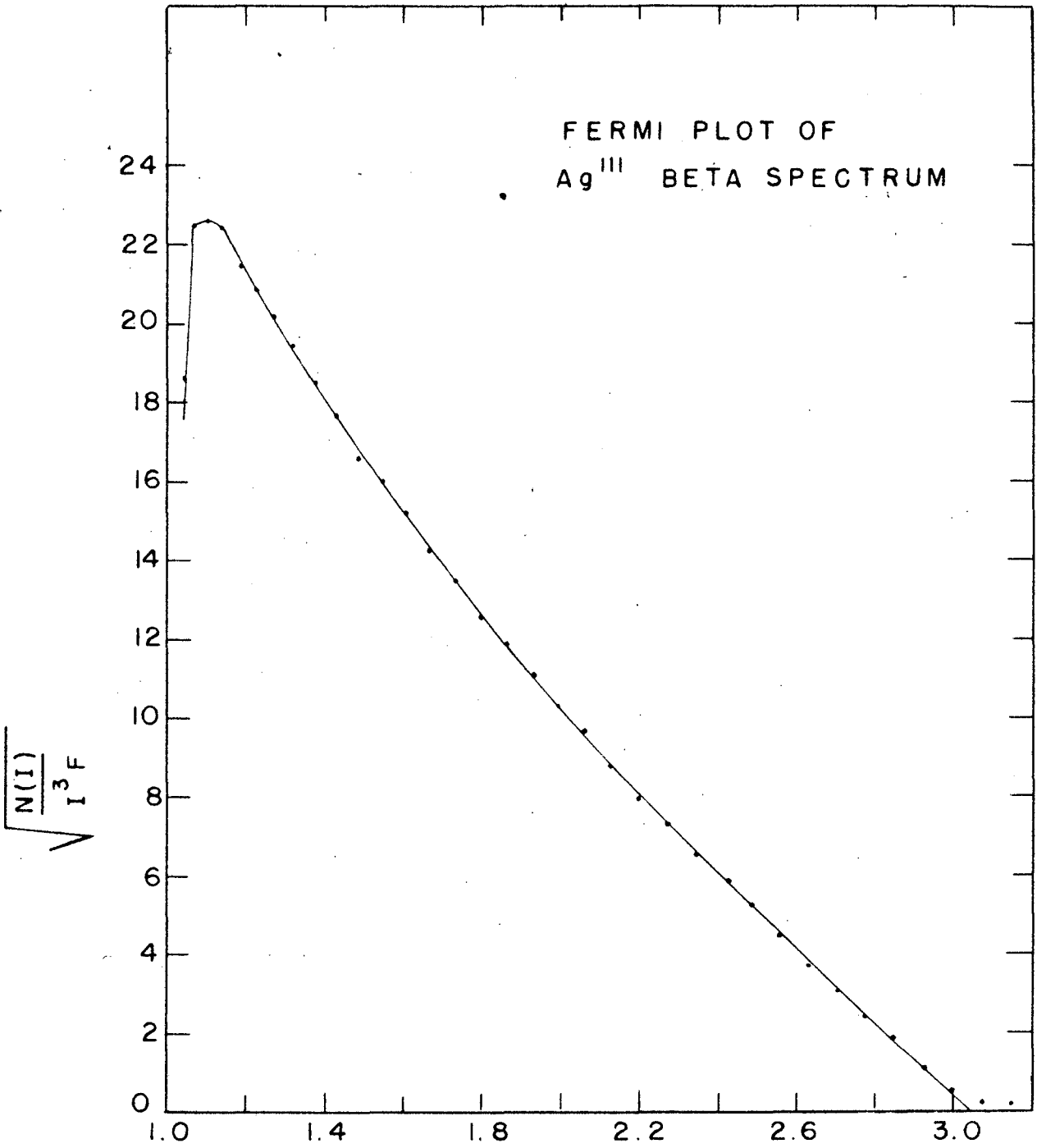


FIG. 21

ground state and the first excited state. However, making the parities the same makes the transition to the ground state allowed. The $f \tau_{1/2}$ value for the Ag^{111} beta spectrum classifies it as a first forbidden transition. So probably there is an additional selection rule operating.

Yttrium 90

As was mentioned earlier the spectra of forbidden transitions may in some cases be expected to have shapes different from those of allowed transitions. The exact form of the momentum distribution in such cases will be determined by the form of the particular interaction between the nucleon and the electron-neutrino field that is assumed. Since the forbidden factor may be dominated by terms which are not dependent on energy or if selection rules other than those on spin and parity operate so as to increase the half-life, it is possible for a once forbidden or twice forbidden spectrum to have an allowed shape. The shape of an allowed spectrum is determined by the statistical distribution of the momentum between the electron and the neutrino and hence gives no direct uniqueness to the form of the interaction. However, a distribution different from an allowed spectrum would be consistent with a theoretical description. Only two types of forbidden spectra have been found to date, notably the RaE spectrum investigated by Neary³³ and a group of elements having the same type of spectra Y^{90} , Sr^{89} , Y^{91} , and Cs^{137} investigated recently by Langer³⁴ and Wu³⁵. The RaE spectrum can be accounted for but the explanation involves considerable arbitrariness in the evaluation of several matrix elements that appear in the forbidden factor. As a result, one cannot come to definite conclusions regarding the type of interaction on the basis of the RaE spectrum.

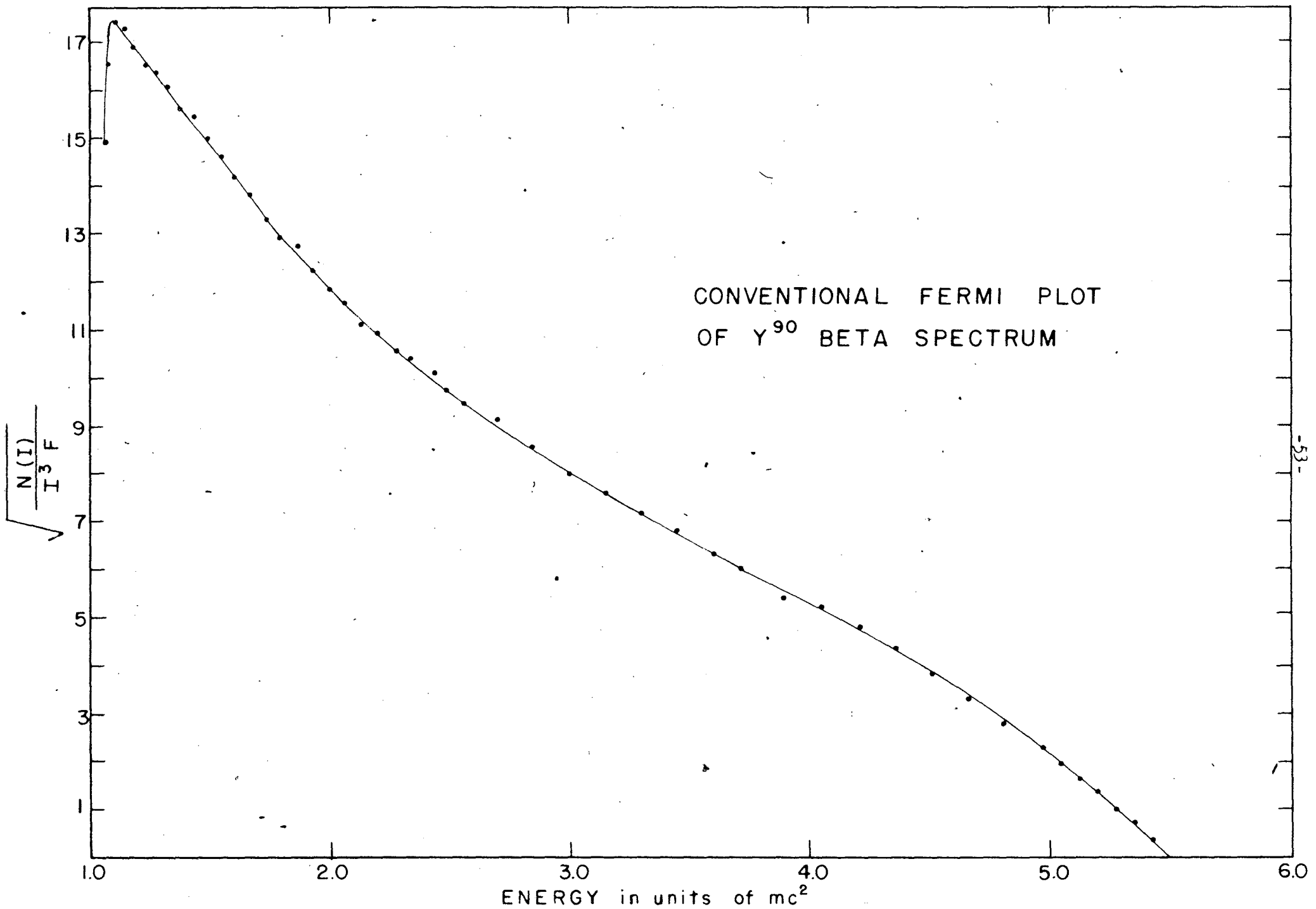
In the tensor interaction (Gamow-Teller selection rules) when the disintegration involves a spin change of one unit higher than the degree of forbiddenness all but one of the nuclear matrix elements vanish so that a unique spectral distribution is predicted. The above four isotopes are all found to have this distribution which lends a great deal of weight to the validity of the Gamow-Teller selection rules especially since the nuclear shell structure analysis of Feenberg and Hammack³⁶ predicts a spin change of two units and a parity change for Y^{91} and Sr^{89} .

The unique energy dependence differs from the allowed shape by the factor

$$p^2 + (W_0 - W)^2$$

where the terms correspond to the squares of the electron's and the neutrino's momenta. If one made a Fermi plot of the spectrum as one does conventionally a deviation from a straight line would be expected. However, if the values of the conventional Fermi plot are divided by the factor $[p^2 + (W_0 - W)^2]^{1/2}$, a straight line should result.

Through the kindness of Dr. J. W. Gofman a sample of Y^{90} ($T_{1/2} = 62$ hours) chemically separated from its beta active parent Sr^{90} ($T_{1/2} = 25$ years) was furnished. The sample was mounted on a film of Formvar forming a source of about 0.1 mg/cm^2 average thickness. The Fermi plot of the spectrum is shown in Figure 22 showing the definite nonlinearity characteristic of this interaction. In Figure 23 the same spectrum has been divided by the factor $[p^2 + (W_0 - W)^2]^{1/2}$ and it is seen that a very good straight line fit is obtained over the major portion of the spectrum. The value of the Y^{90} end point is 2.30 ± 0.02 Mev which is slightly higher than that observed by Langer³⁴.



ENERGY in units of mc^2
FIG. 22

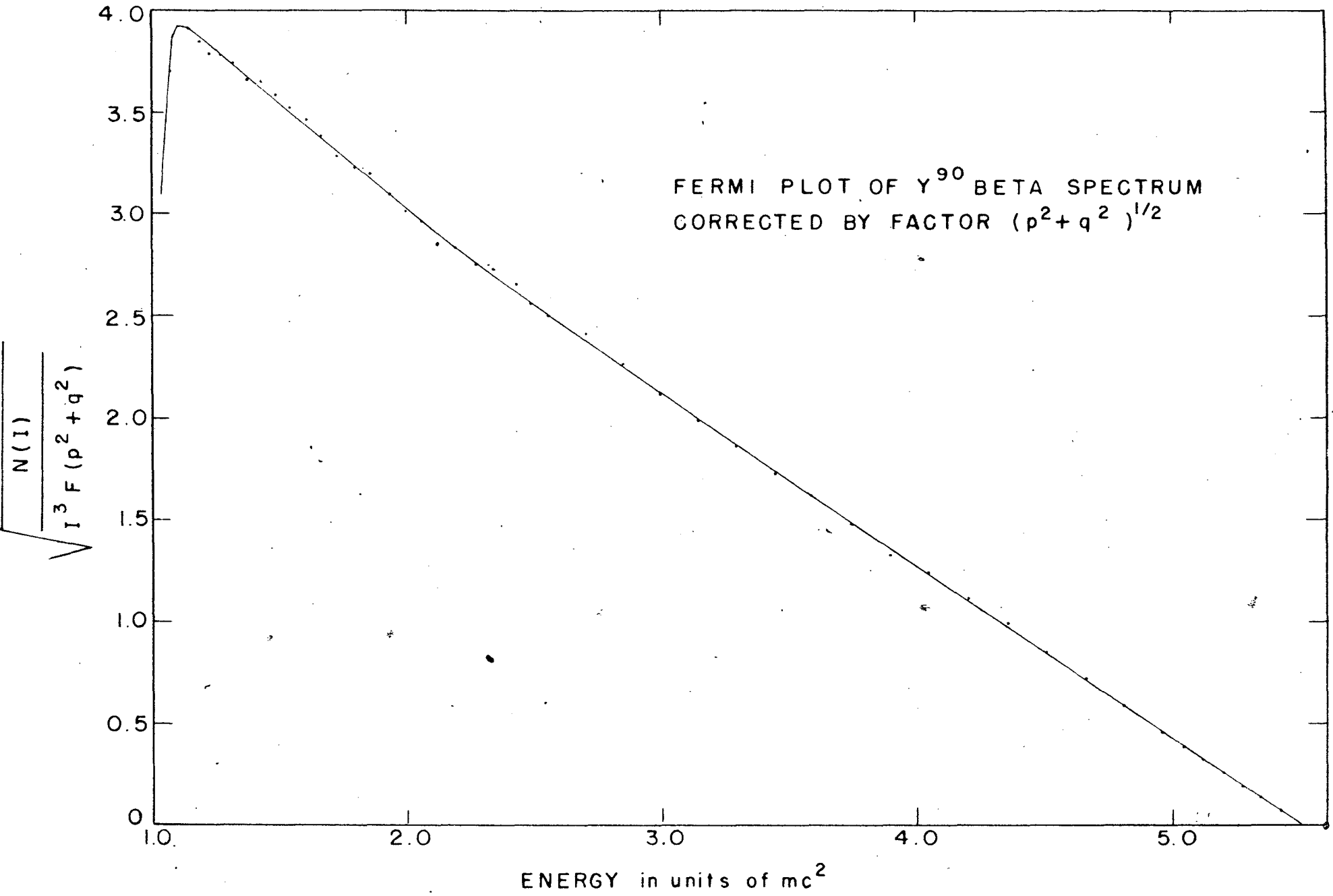


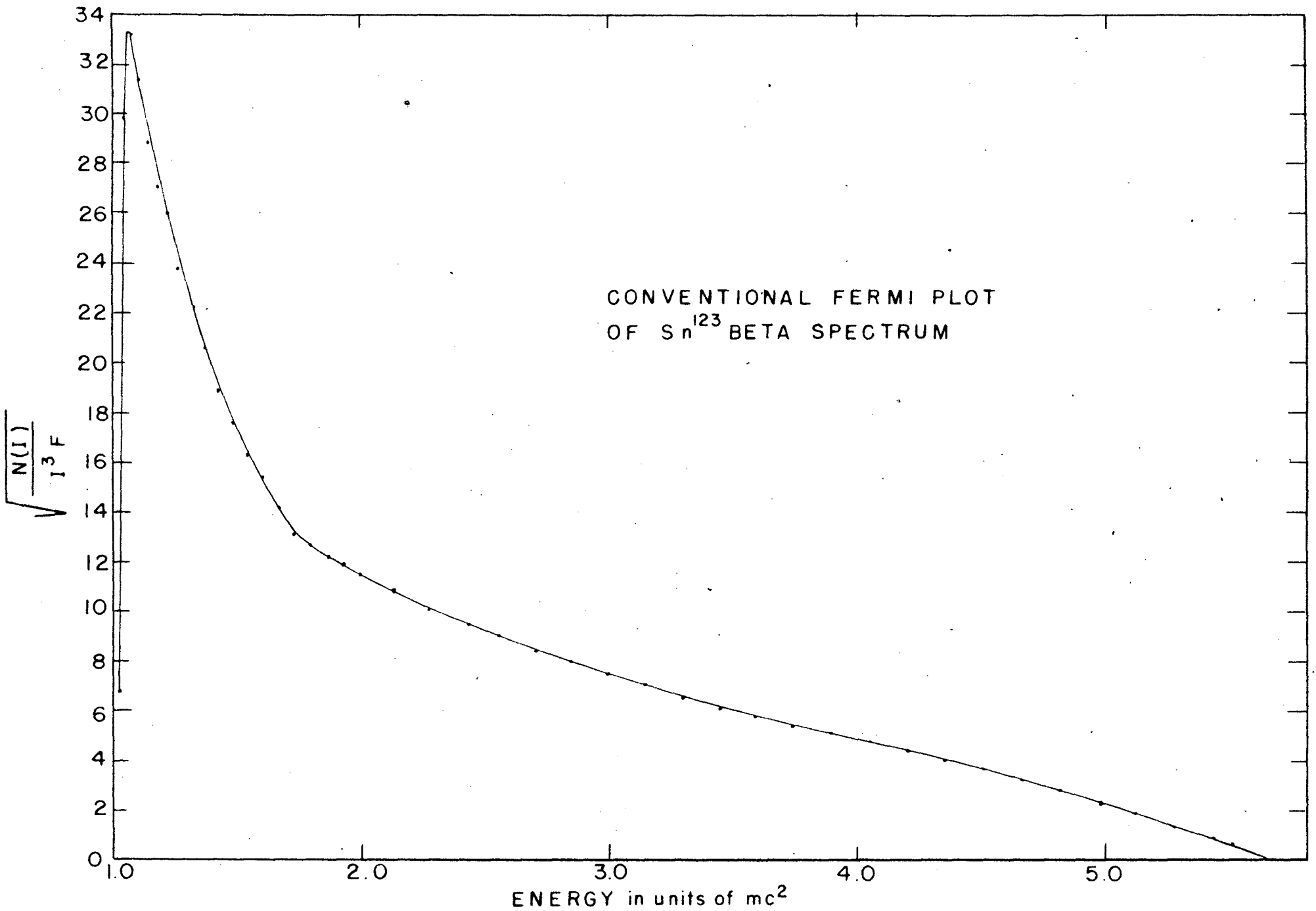
FIG. 23

Tin 123

The 9.5 day tin activity has been tentatively assigned to Sn^{123} by Newton and McDonell³⁷ by the bombardment of enriched isotopes of tin by deuterons with the 60-inch Berkeley cyclotron. This assignment may be open to some question since three isomers must be placed at Sn^{123} . Besides the 9.5 day period a 39 minute beta period has been observed with an upper energy of about 1.7 Mev accompanied by a 0.17 Mev gamma and the antimony x-rays indicating that the 39 minute activity decays to an excited state of Sb^{123} followed by gamma emission to the ground state, the gamma being partially converted. Another activity assigned to Sn^{123} is a 130 day period with a beta energy of about 1.5 Mev and no gamma.

Absorption in aluminum³⁷ of the 9.5 day period indicated the presence of a gamma-ray corresponding to 0.4 percent of the total radiation, low for a gamma-ray unless it is highly converted. Lead absorption curves on this radiation indicated the possible presence of a 1.5 Mev gamma.

A sample of the 9.5 day tin made by fission of thorium with deuterons and separated with 50 micrograms of carrier was furnished by Dr. A. S. Newton. The beta spectrum was investigated by mounting a small portion of the sample on a nylon film 0.4 mg/cm^2 , the film accounting for the major thickness of the sample. A Fermi plot of the beta spectrum is shown in Figure 24. It was noted that this spectrum has the same general shape as the forbidden spectrum of Y^{90} . The $f\tau_{1/2}$ value of 3.7×10^8 for the 9.5 day tin indicates that the spectrum is in the second forbidden classification as is Y^{90} . Division of the conventional Fermi plot by the factor $\left[p^2 + (W_0 - W)^2 \right]^{1/2}$ gives the Fermi plot shown in Figure 25. A straight line relationship is now obtained for the larger portion of the spectrum. A low energy beta spectrum is present, being about ten percent of the intensity of the higher energy spectrum.



CONVENTIONAL FERMI PLOT
OF Sn^{123} BETA SPECTRUM

FIG. 24

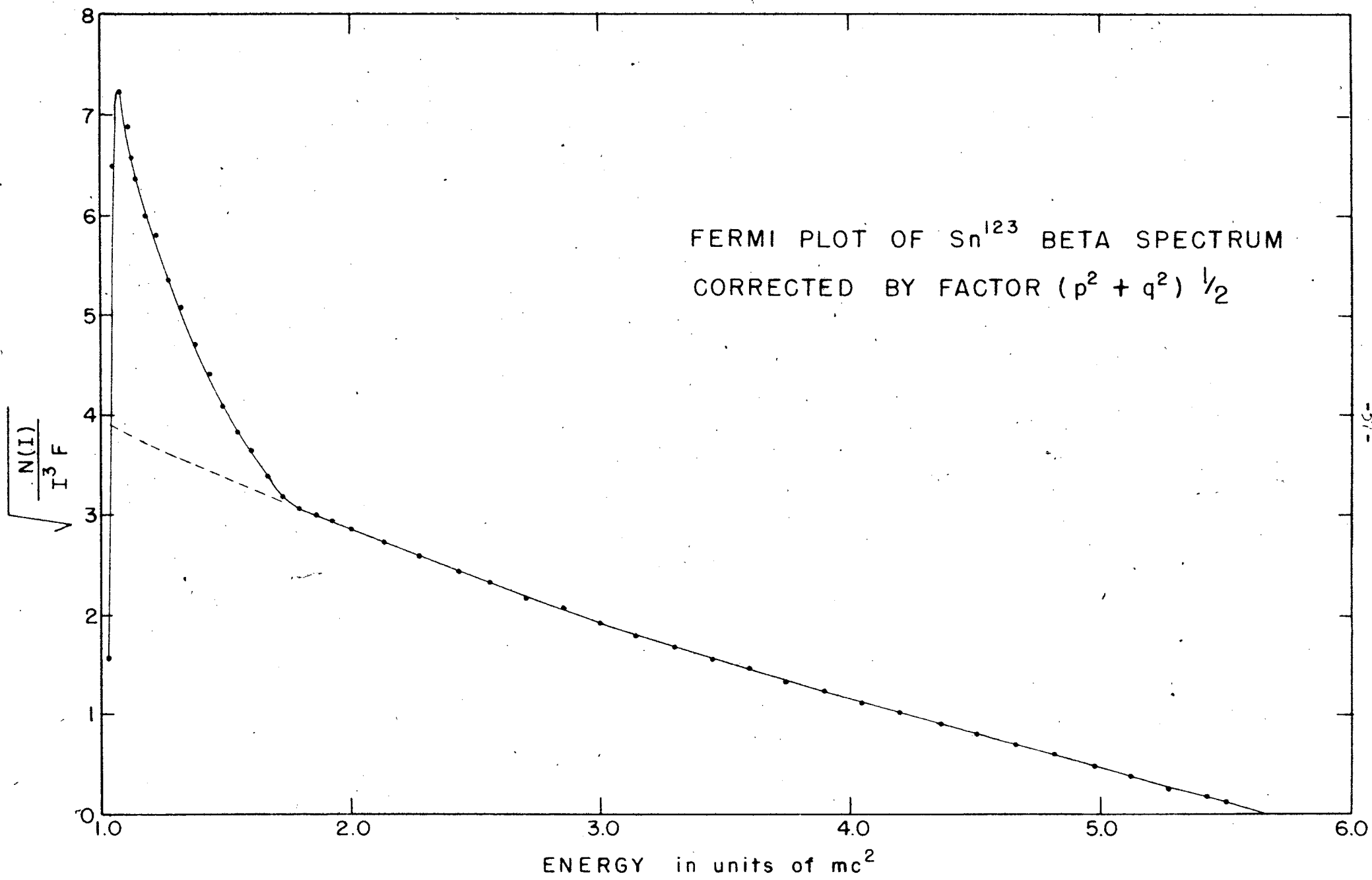


FIG. 25

Both spectra appear to decay with the same lifetime. In Figure 26 is the Fermi plot of the low energy component when the extrapolated contribution of the high energy distribution is subtracted out. The values of the upper energy limits for the two beta spectra are 2.38 ± 0.02 and 0.400 ± 0.008 Mev. The remainder of the sample was placed in a copper radiator and a search was made for the Compton electrons from any gamma radiation present. The results were negative indicating that if there is any gamma radiation present it is extremely weak.

The fact that this spectrum has a forbidden shape is in agreement with the $f \gamma_{1/2}$ value. The shape could hardly be attributed to such things as source thickness or resolving power, the major differences between beta spectrographs. Wu³⁸ has made experiments with Y^{91} varying these two quantities. Increasing the source thickness tended to straighten out the Fermi plot because of greater back scattering at the low energies. Varying the resolving power had no effect on the shape.

Little significance can be put on the curved shape of the low energy component since the subtraction process is subject to large errors. The back scattering of the high energy spectrum is not taken into account, hence a small number of scattered electrons will appear tenfold in the low energy component. It is most puzzling that there is no gamma radiation when a branching ratio this large is observed. Attempts to separate an antimony daughter from the 9.5 day activity set a lower limit to the antimony half-life of 200 years³⁷.

Cadmium 116

The 2.33 day activity of cadmium was found by Cork and Thornton³⁹ who bombarded cadmium with deuterons. They found that chemically separated cadmium increased in activity for a short time before beginning to decay. Subsequent separations of indium from the cadmium showed that the activity

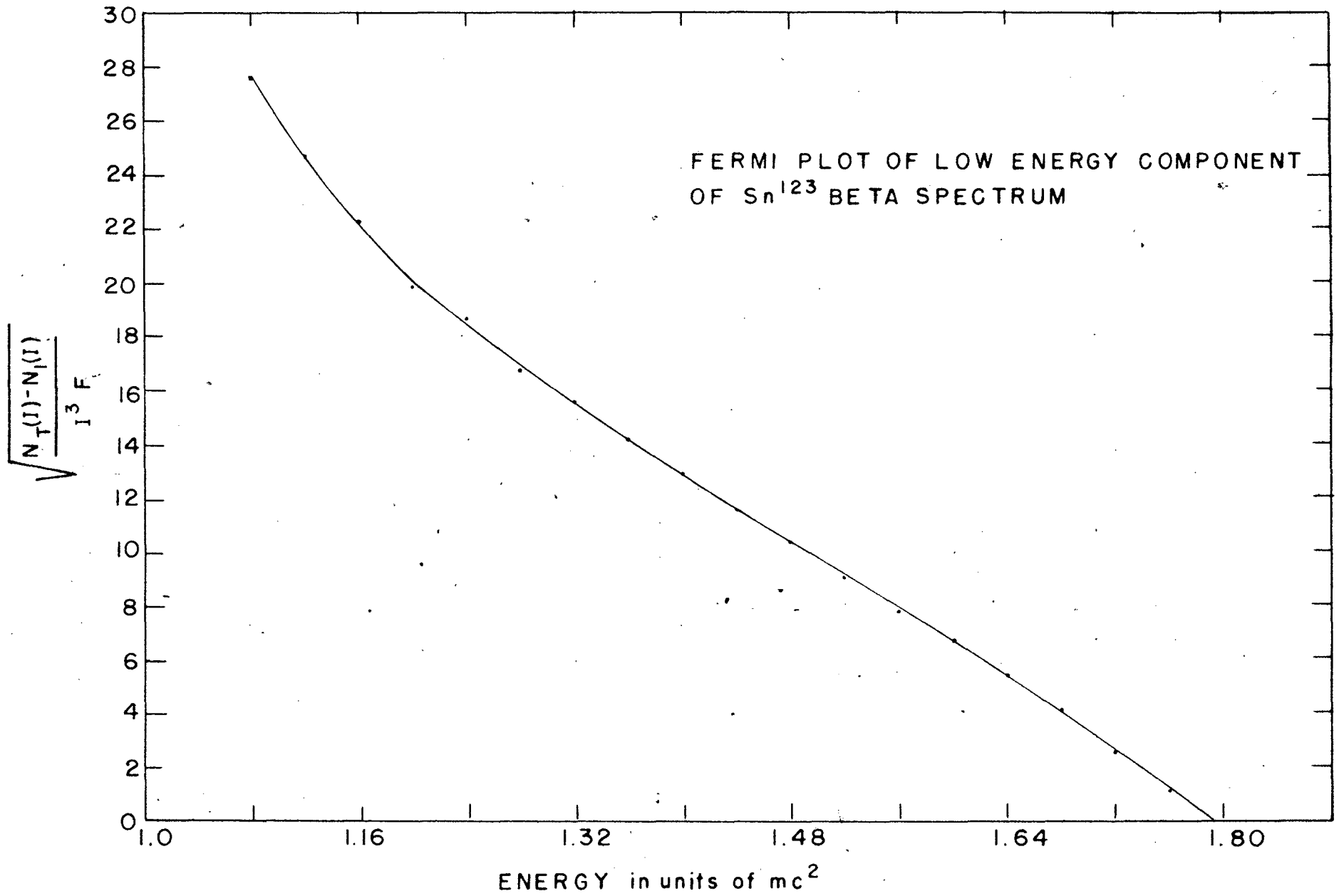
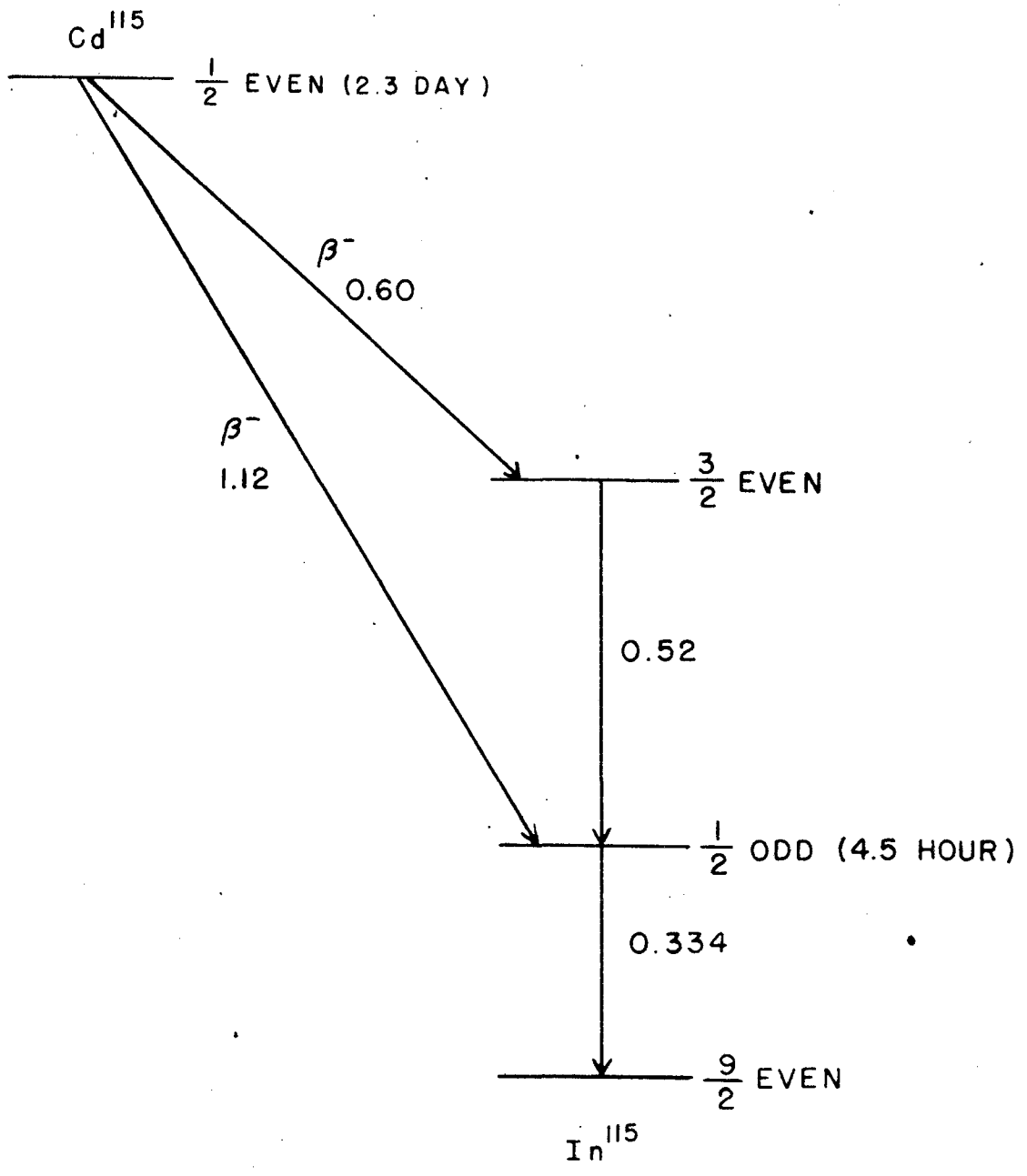


FIG. 26

decayed with a half-life of 4.5 hours. This is the well known isomer of In^{115} . Lawson and Cork⁴⁰ investigated the beta spectrum of Cd^{115} and found what appears to be a complex beta spectrum with $E_0 = 1.13$ Mev. In addition two gamma-rays were found. The first was highly converted and corresponded to the 0.337 Mev gamma observed in the 4.5 hour indium. The other gamma was much weaker and had an energy of 0.54 Mev. They postulated a decay scheme shown in Figure 27.

In the course of the investigation of the 43 day Cd^{115} a sample of the 2.33 day Cd^{115} was prepared. This was done by a (d,p) reaction on cadmium necessitating a sample of several mg/cm^2 thickness because of the low specific activity. The beta spectrum shown in Figure 28 is essentially the same as that observed by Lawson and Cork. The conversion line has an energy of 0.306 Mev giving a gamma-ray energy of 0.334 ± 0.006 Mev. A Fermi plot was made of the portion of the spectrum not obscured by the strong conversion line and is shown in Figure 29. There are two discontinuities corresponding to the two end points of the 2.33 day Cd^{115} beta spectrum. The high energy portion of the Fermi plot goes with the 43 day Cd^{115} isomer. The upper limit of the beta spectrum to the isomeric state is 1.12 ± 0.03 Mev while the low energy beta component has an upper energy of 0.55 ± 0.10 Mev. The poor resolution of this value is due mainly to the thick source. A photoelectron spectrum using a gold radiator of 10 mg/cm^2 thickness is shown in Figure 30. The energies of the K and L photoconversion peaks are 252.0, 313.1, 442.6, and 511.0 Kev. The first two correspond to a gamma-ray of 0.334 ± 0.006 Mev and the latter two correspond to a gamma-ray energy of 0.523 ± 0.010 Mev. These values are lower but agree within the probable error with the values of Lawson and Cork. The beta transitions to the two upper



DECAY SCHEME OF Cd^{115} (2.3 DAY)

FIG. 27

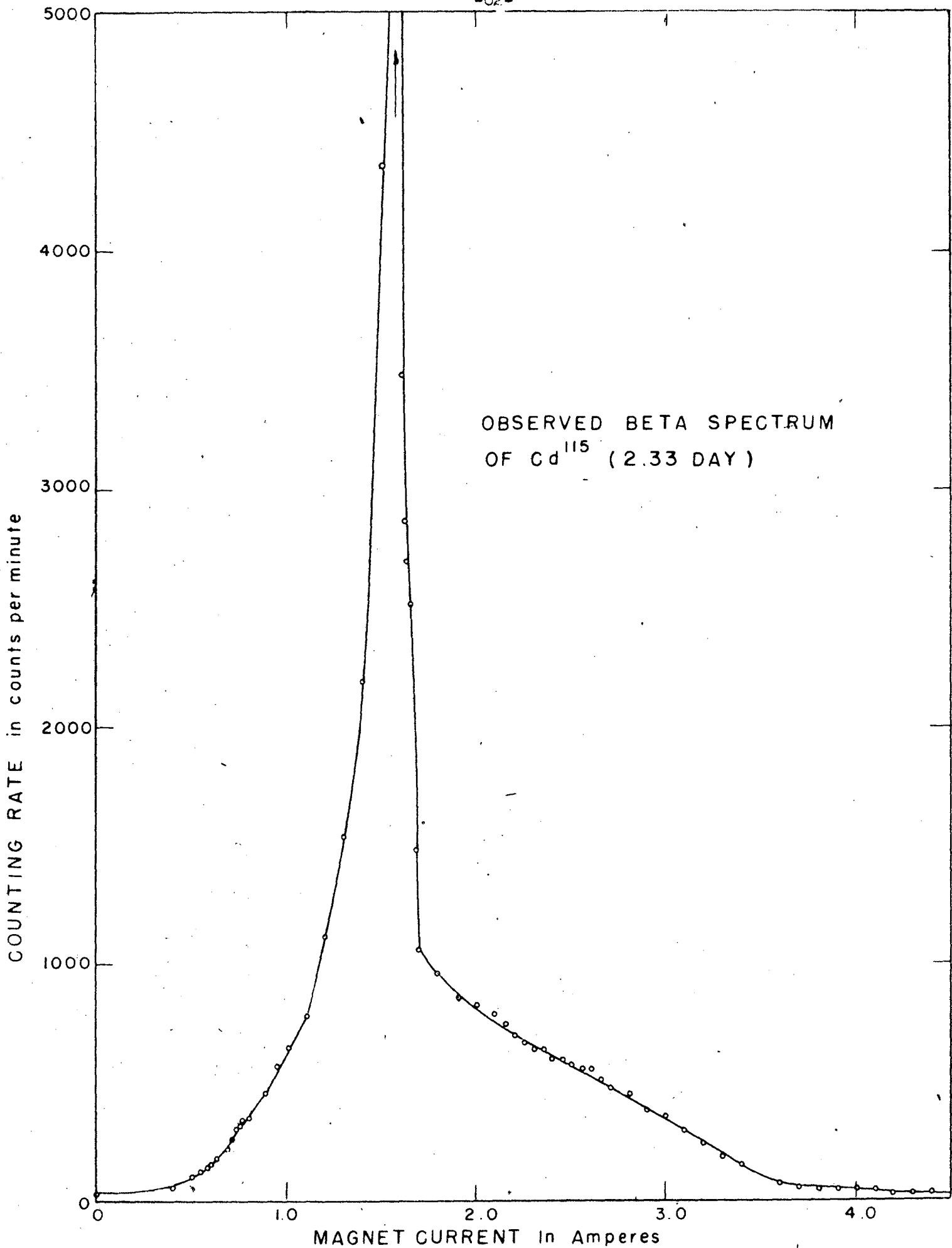


FIG. 28

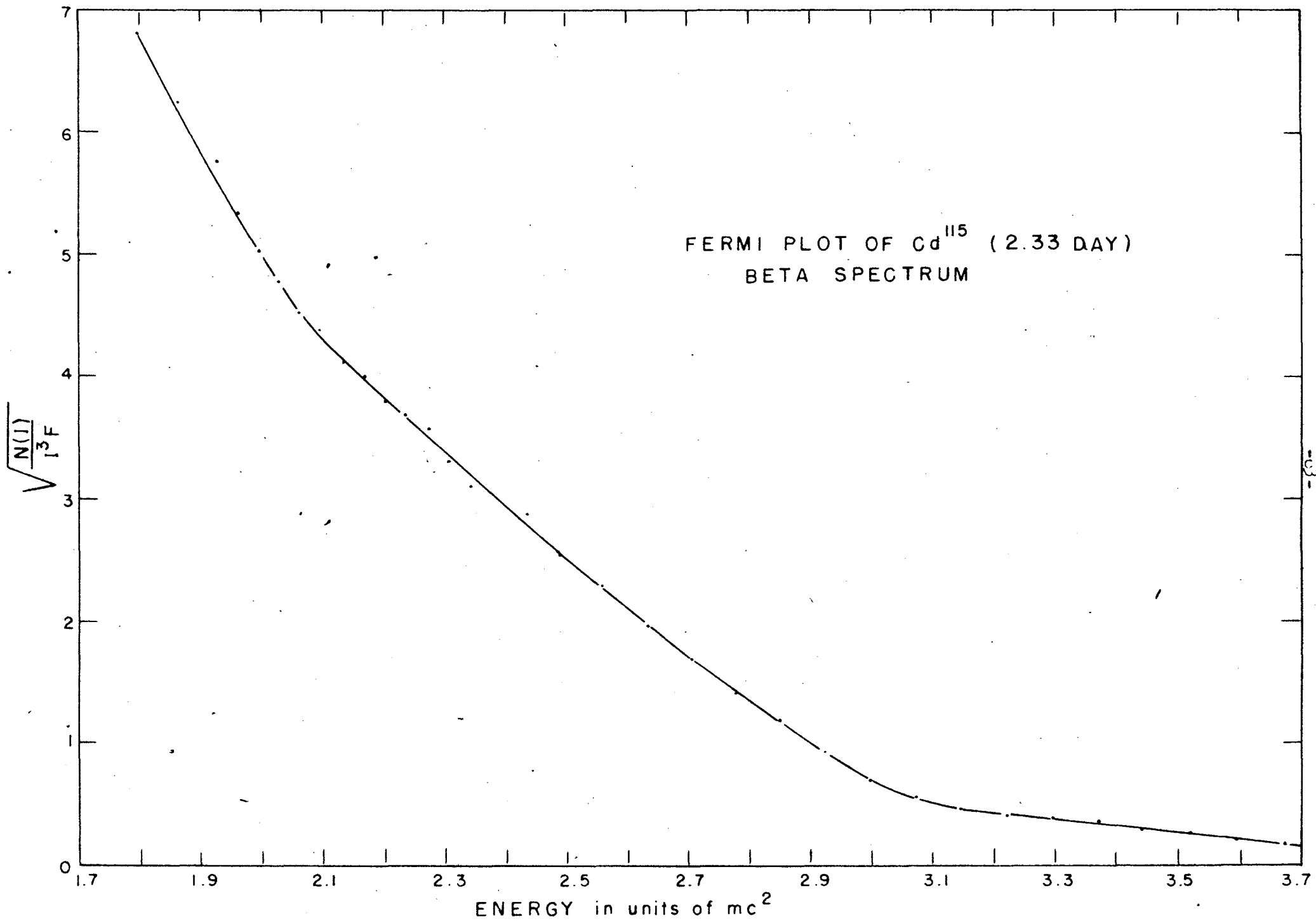


FIG. 29

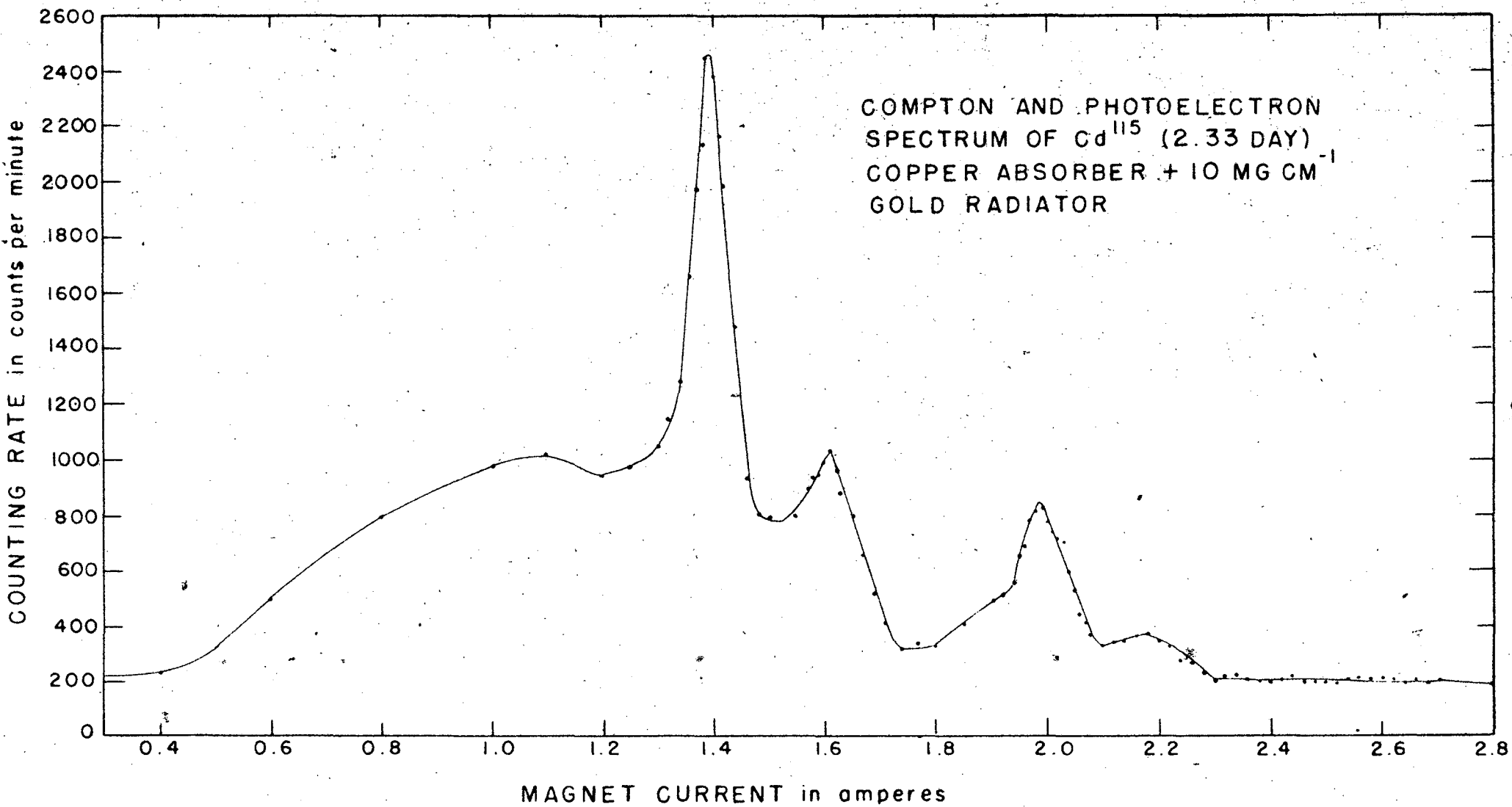


FIG. 30

states of In^{115} probably have the same degree of forbiddenness. The $f \tau_{1/2}$ value of the Cd^{115} beta is 8.6×10^6 indicating a first forbidden spectrum. The higher energy component of the beta spectrum can be first forbidden and the lower energy component can be allowed, but because of the strong energy dependence of the transition probability the transitions will be slightly favored along the first forbidden path. Since the 0.523 Mev gamma is not converted it is probably a simple dipole radiation. The lifetime of the 4.5 hour state together with the transition energy of 0.334 Mev indicate according to the classification of Axel and Dancoff¹¹ a change in angular momentum of 5 requiring a spin change of at least 4 and a parity change. Using these data one can construct a level scheme with spins and parities that will be consistent with observation. One assumes even parity for the ground state of In^{115} and the spin has been measured to be $9/2$. The first excited state could have a spin of $1/2$ and odd parity and the next excited state above it can have a spin of $3/2$ and even parity. In order to make the beta transition to the 4.5 hour state in In^{115} first forbidden and allowed to the next higher state, the spin should be $1/2$ with even parity. The level scheme agrees with that proposed by Lawson and Cork.

The 43 day activity in Cd^{115} was first reported by Cork and Lawson⁴¹ who noticed a long lived activity after the 2.33 day component had died out. This activity was assigned definitely to Cd^{115} by Seren and co-workers⁴² by bombardment of cadmium with slow neutrons and by n,p reactions on indium. To investigate this isomeric activity a sample was obtained from Oak Ridge. The sample consisted of a millicurie of Cd^{115} in several grams of cadmium metal. Because of this low specific activity a source of considerable thickness (10 to 20 mg/cm^2) was required. The beta spectrum is shown in

Figure 31. The two conversion lines at the low current are due to a Cd^{109} contamination of the sample. The Cd^{109} is a K capture activity decaying to the Ag^{109} isomer which emits conversion electrons corresponding to a 86 Kev transition. There is a very small conversion peak corresponding to the 0.334 Mev gamma-ray. If one assumes that this gamma-ray is about 50 percent converted, then comparison of the area under the peak with that of the total beta spectrum indicates that about 10^{-4} of the disintegrations go through the 4.5 hour isomeric state of In^{115} . A Fermi plot of the beta spectrum of Cd^{115} is shown in Figure 32. The large curvature at the low energy portion is due mainly to the source thickness which introduces considerable back scattering. However, a branching ratio is indicated by the presence of the 0.334 Mev conversion line and this would account for the presence of the lower energy components. The upper limit of the beta spectrum is 1.65 ± 0.02 Mev. This value would place the 43 day Cd^{115} isomer above the 2.33 Cd^{115} isomer by 0.2 Mev. Since no evidence for such a gamma-ray has been found the gamma transition must correspond to at least a 2^6 and probably a 2^6 pole transition. This would require that the spin of the 43 day Cd^{115} would be $13/2$ and its parity even. This agrees with the fact that the transition to the ground state of In^{115} is second forbidden. The assignment of spins to the two isomeric states is also in agreement with the fact that in the reaction $\text{Cd}^{114} (n, \gamma) \text{Cd}^{115}$ with thermal neutrons the cross section of the 2.3 day period is eight times that for the 43 day period¹⁰. The decay scheme is shown in Figure 33. Recent work still in progress indicates that there are other levels in In^{115} . One level has been found 0.225 Mev above the highest level in Figure 23. Evidence consists in the observation of photoelectrons from a 40 mg/cm²

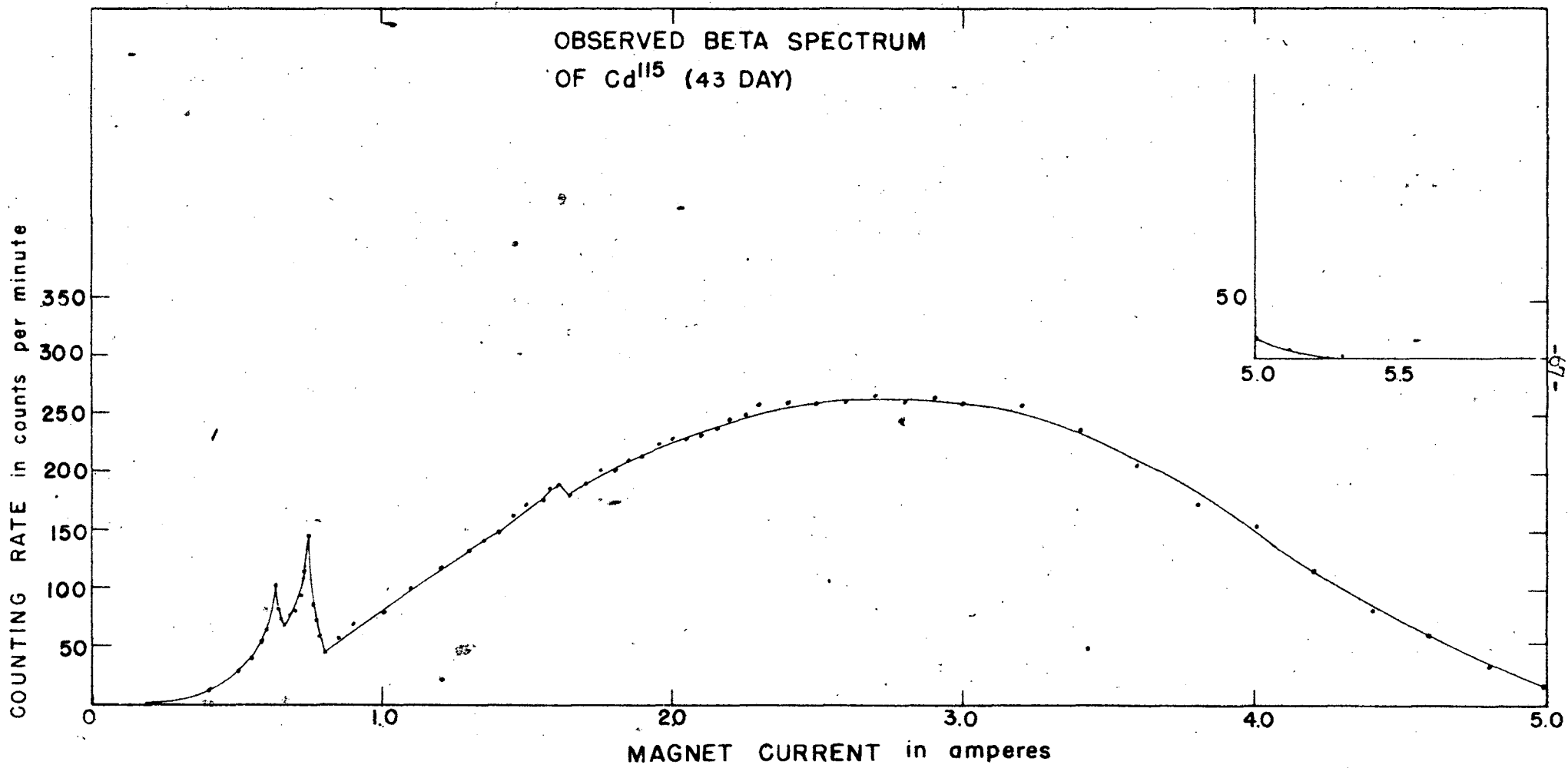


FIG. 31

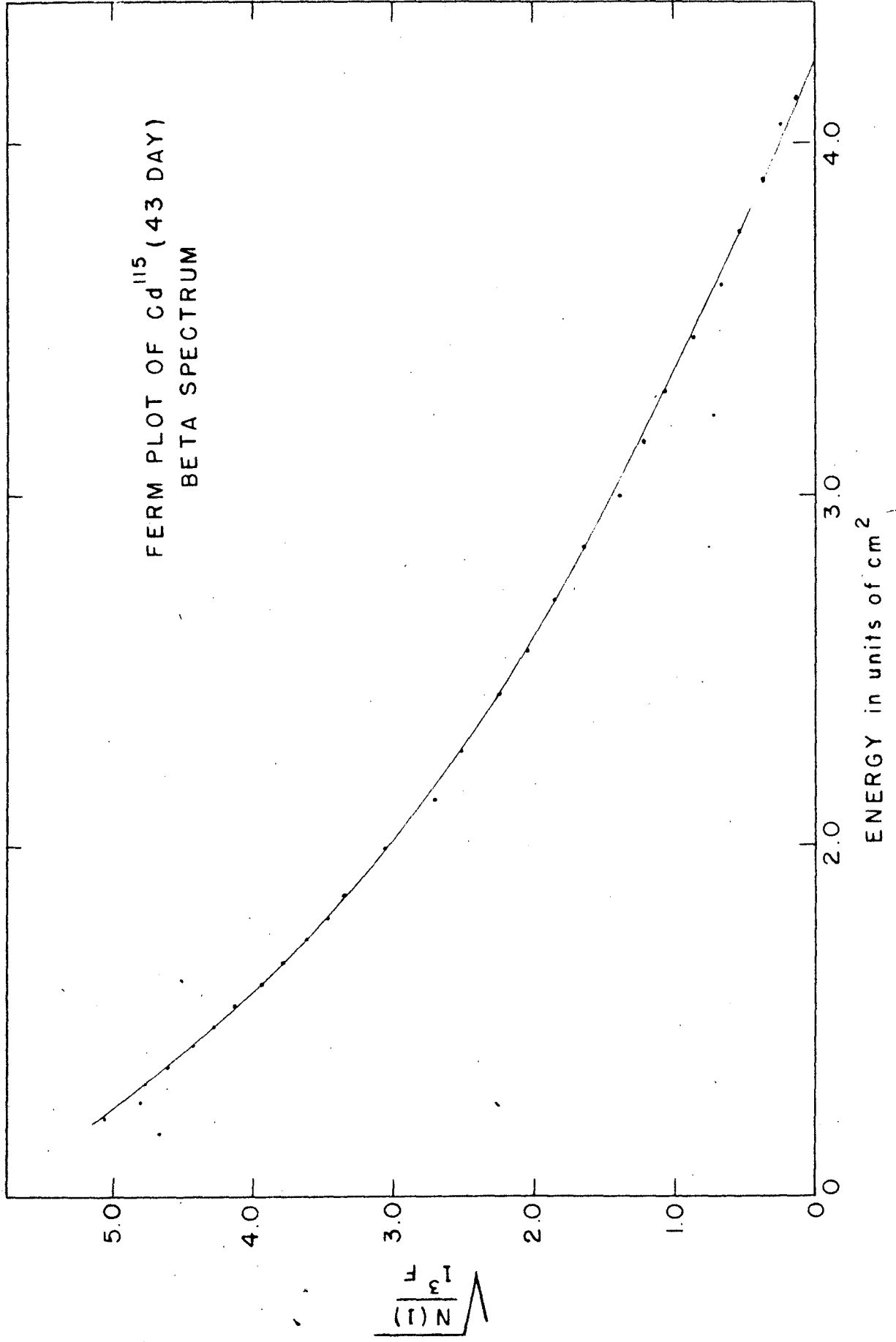
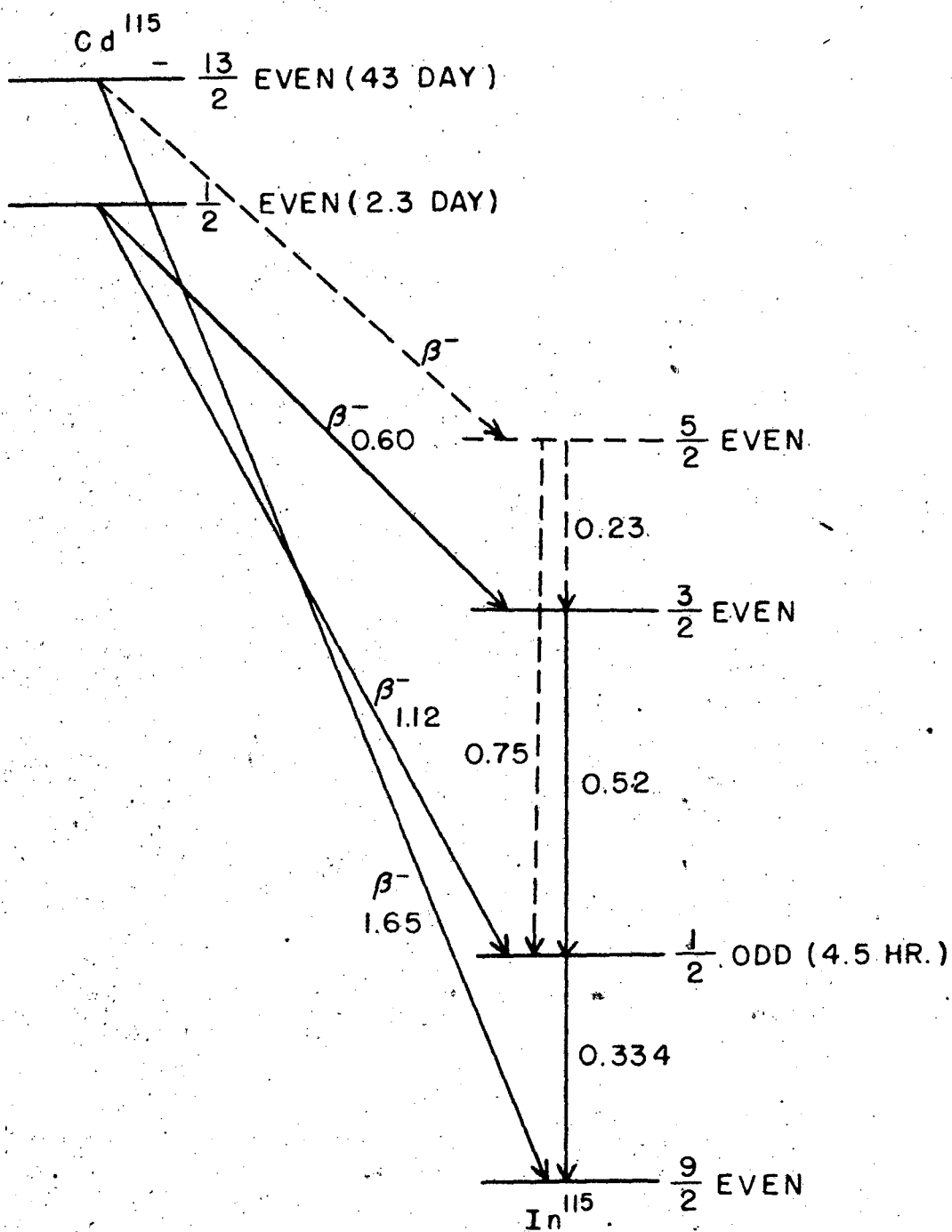


FIG. 32



DECAY SCHEME OF Cd^{115} 43 DAY

FIG. 33

uranium radiator corresponding to gamma-ray energies of 0.23 Mev and a cross over gamma-ray of 0.75 Mev which is the sum of the 0.23 and the 0.52 Mev transitions. These energies are consistent with levels found by Waldman⁴³ by excitation of Indium with x-rays. He finds levels of 0.87 Mev and 1.02 Mev above the ground state. The cross section of the latter level is much larger. Since he observes no direct excitation of the 0.354 Mev level one can say that the spin of the 1.02 Mev level is half-way intermediate between those of the ground state and the 4.5 hour level. Other radiations not yet correlated have been found.

Acknowledgments

In conclusion I wish to express my thanks especially to Professor A. C. Helmholtz for his continued interest and suggestions regarding the problem and, in a number of instances, for making the bombardments and chemical separations for me. I also wish to thank the Radiation Laboratory for making their facilities available to me. Finally I wish to express gratitude to the Atomic Energy Commission for financial assistance.

Appendix

The following six figures contain schematic diagrams of the electronic circuits developed expressly for use with the beta spectrometer described in this paper.

Figure 34 - Schematic Diagram of Generator Field Supply

Figure 35 - Schematic Diagram of D.C. Amplifier

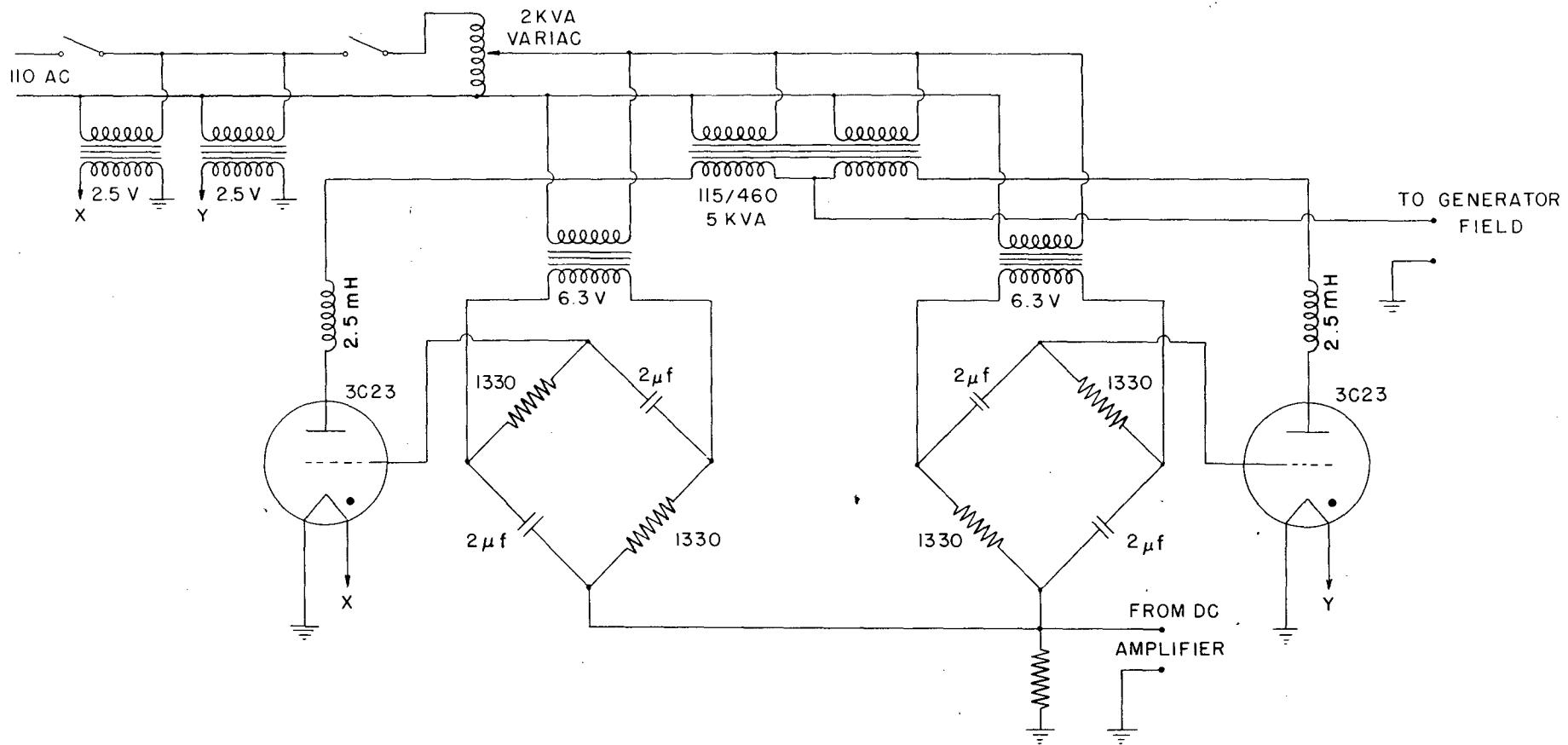
Figure 36 - Schematic Diagram of Geiger Counter Preamplifier

" " " Scintillation Counter
Preamplifier

Figure 37 - Schematic Diagram of Pulse Amplifier

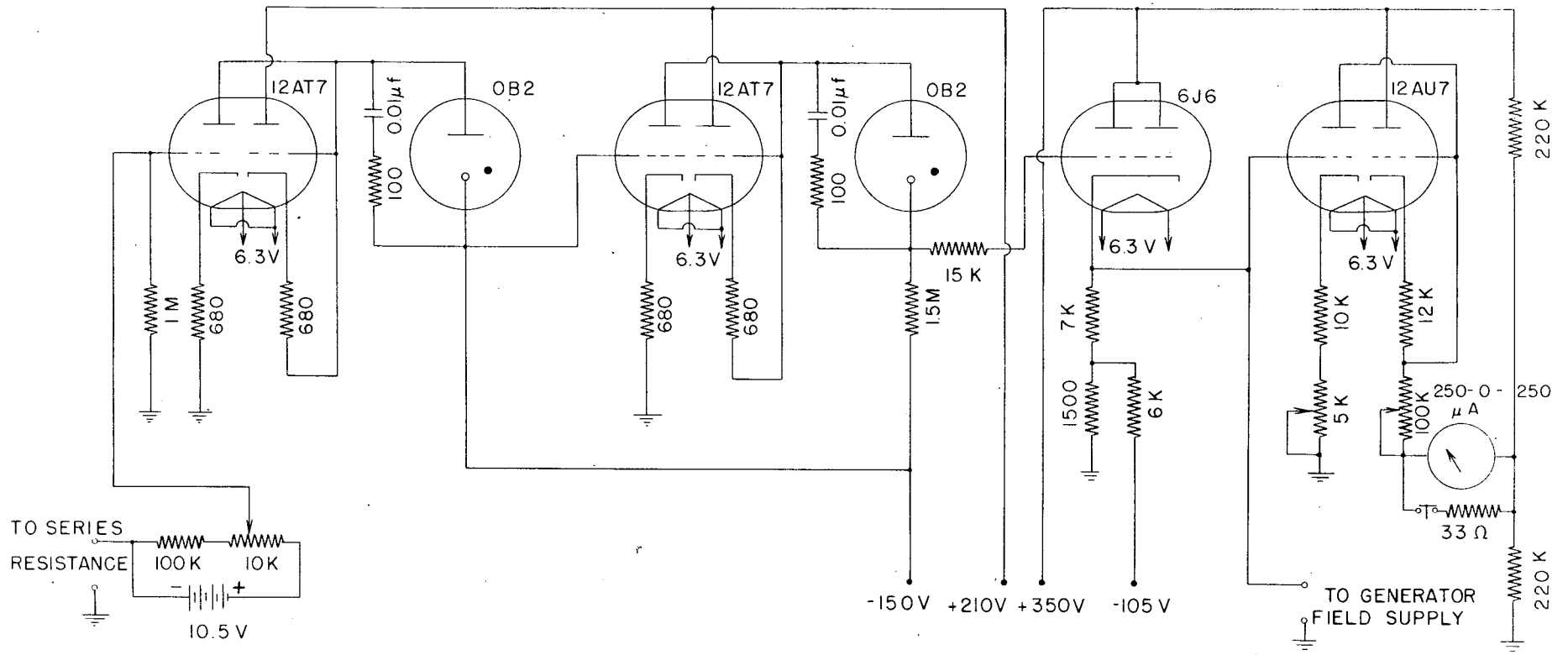
Figure 38 - Schematic Diagram of Coincidence Circuit

Figure 39 - Schematic Diagram of Counting Rate Meter



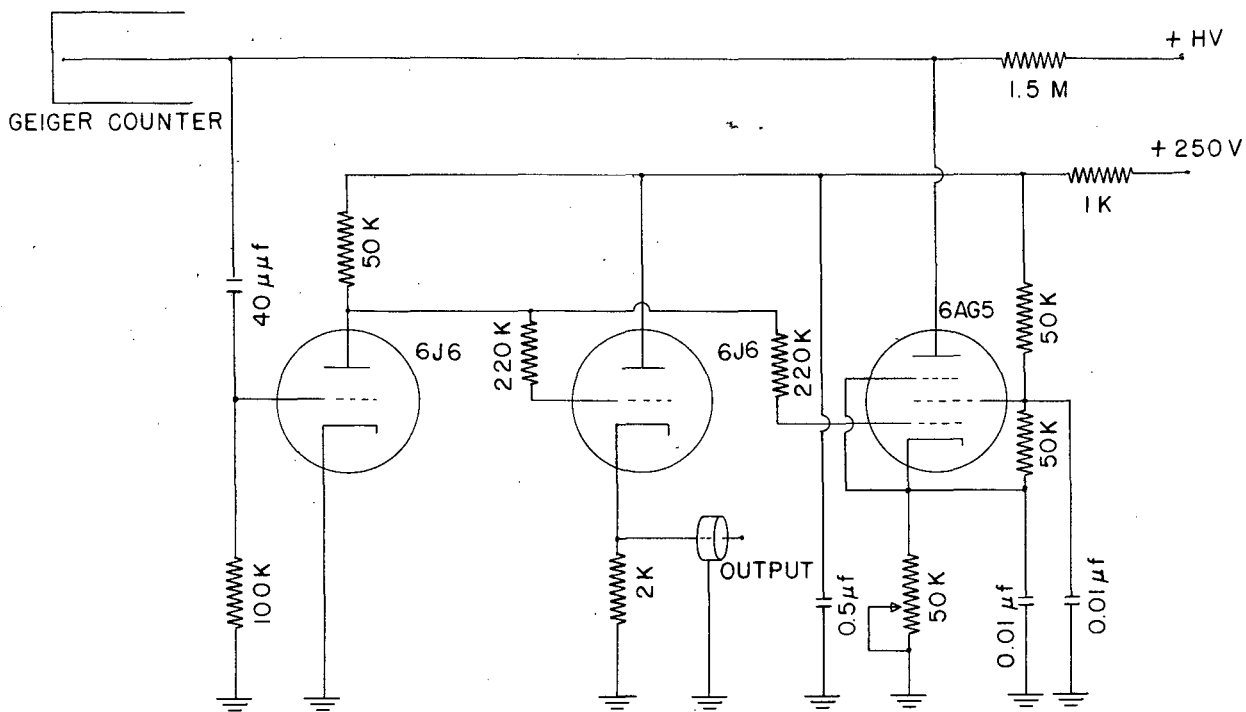
SCHEMATIC DIAGRAM OF GENERATOR FIELD SUPPLY

FIG. 34

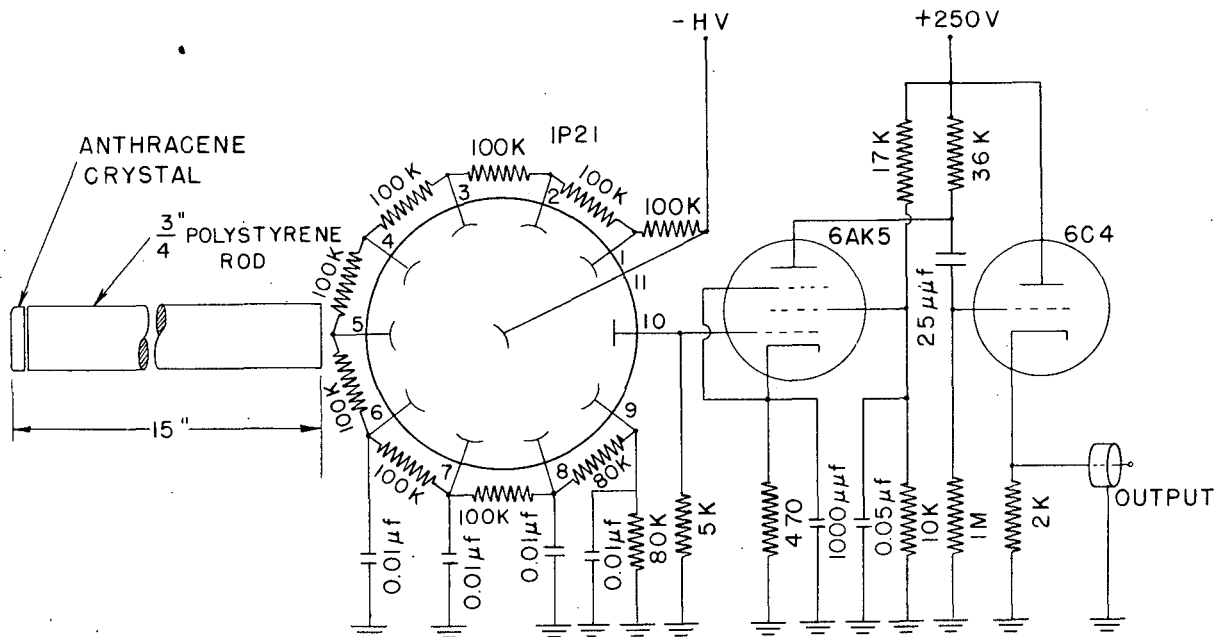


SCHEMATIC DIAGRAM OF DC AMPLIFIER

FIG. 35

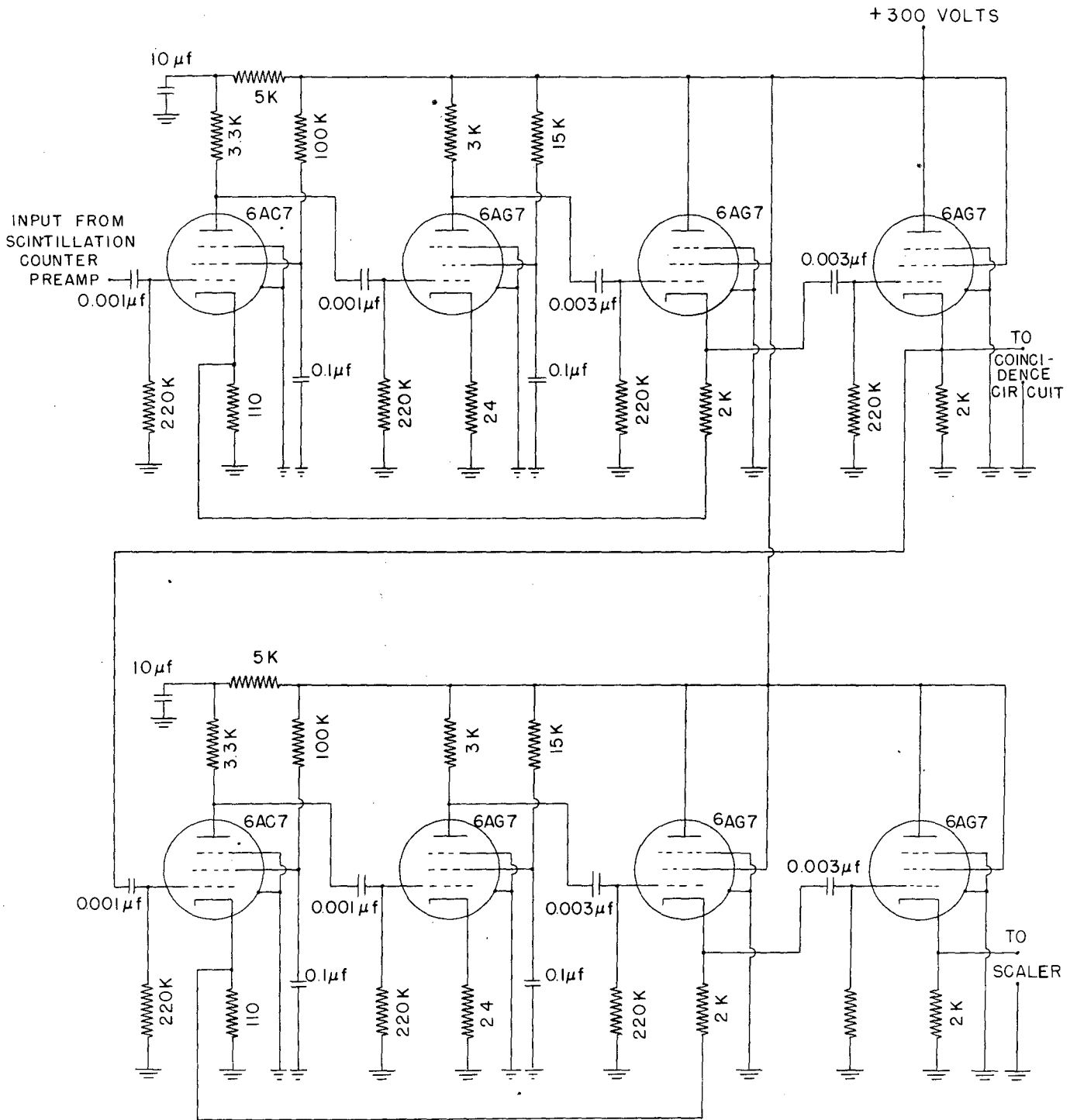


SCHEMATIC DIAGRAM OF GEIGER COUNTER PREAMPLIFIER



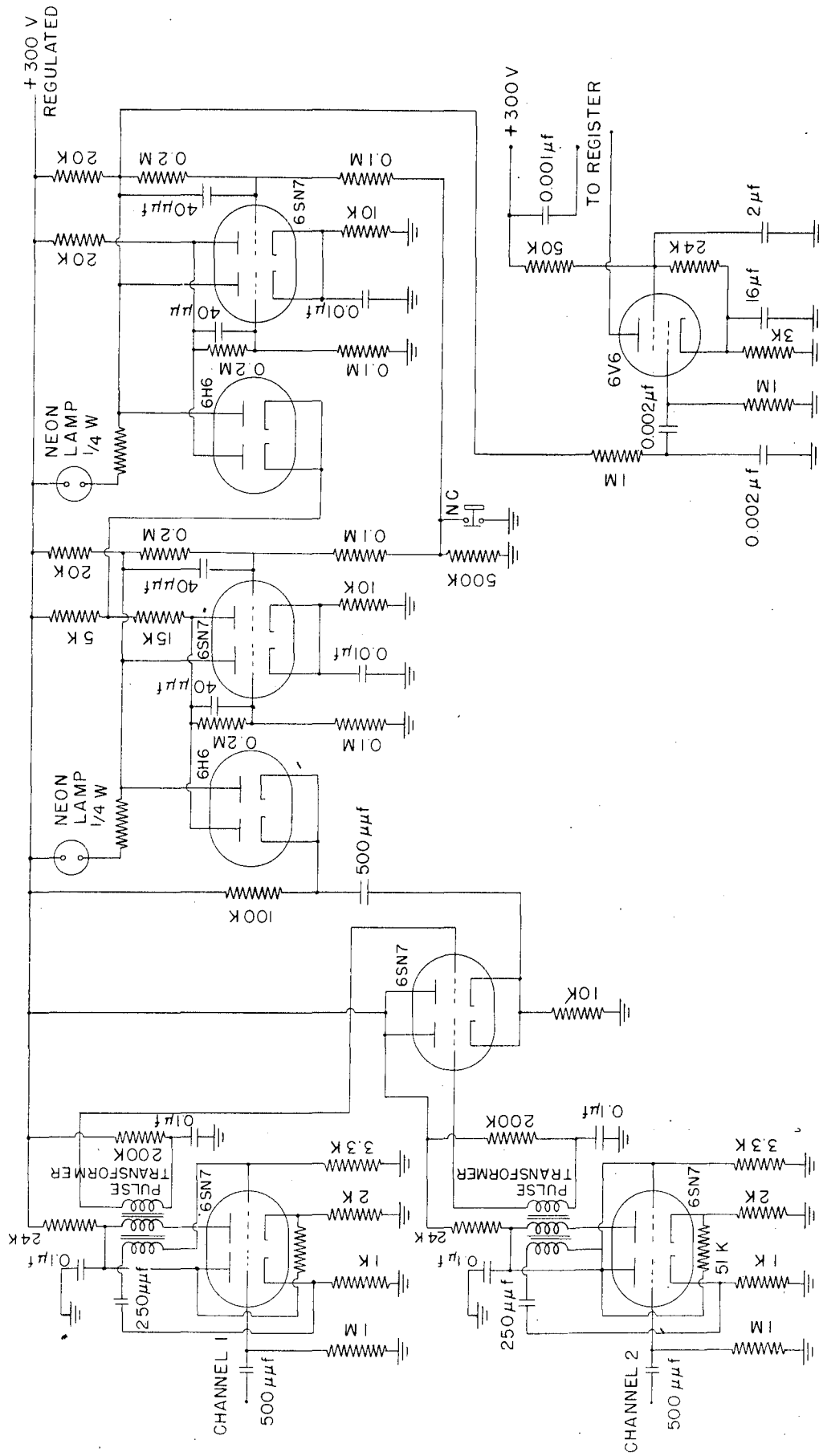
SCHEMATIC DIAGRAM OF SCINTILLATION COUNTER AND PREAMPLIFIER

FIG. 36



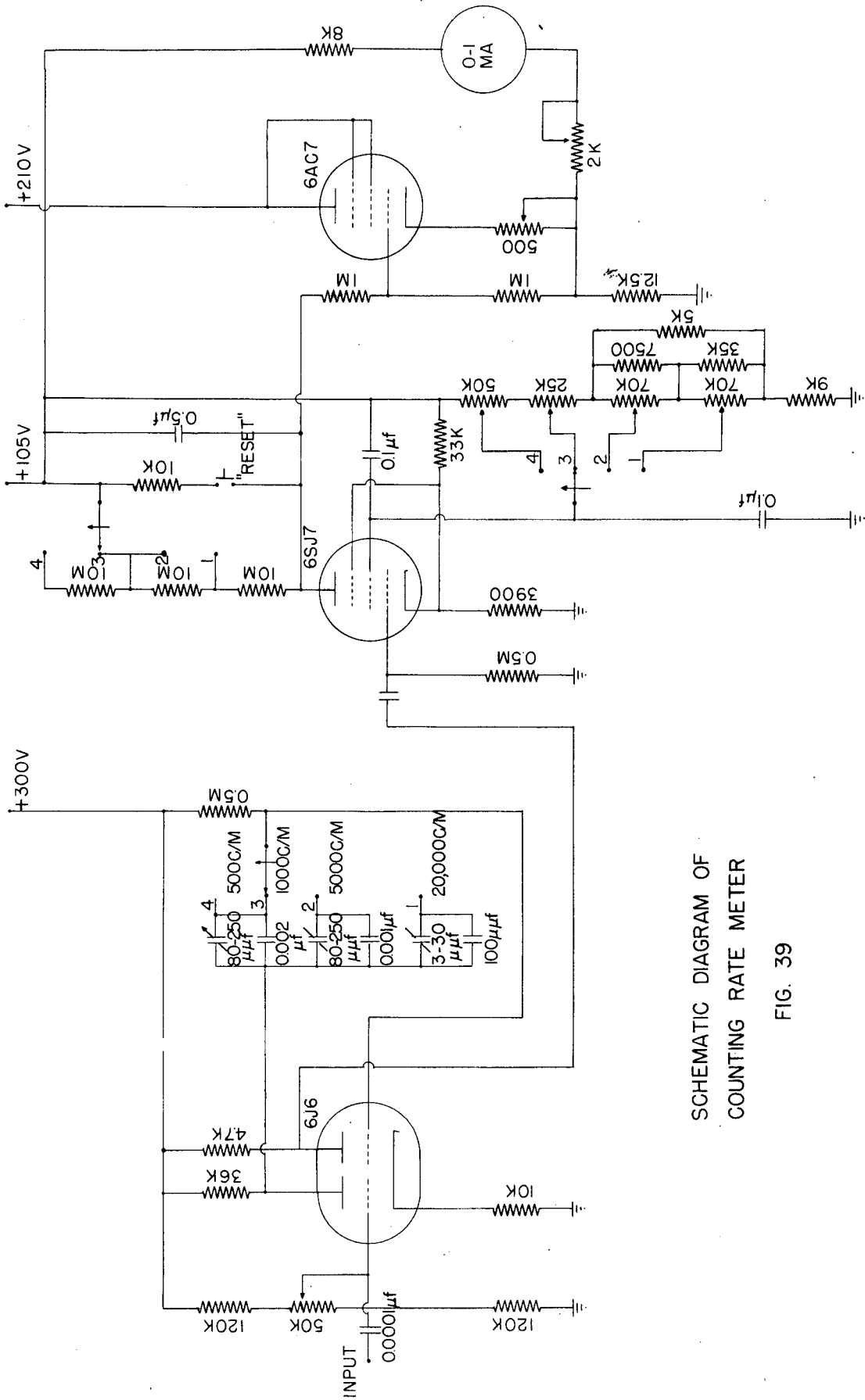
PULSE AMPLIFIER

FIG. 37



SCHEMATIC DIAGRAM
OF COINCIDENCE CIRCUIT

FIG. 38



SCHEMATIC DIAGRAM OF
COUNTING RATE METER

FIG. 39

Bibliography

1. G. T. Seaborg and I. Perlman, Rev. Mod. Phys. 20, 585 (1948)
2. E. Fermi, Zeit. f. Physik 88, 161 (1934)
3. E. J. Konopinski, Rev. Mod. Phys. 15, 209 (1943)
4. G. Gamow and E. Teller, Phys. Rev. 49, 895 (1936)
5. E. Wigner, Phys. Rev. 56, 519 (1939)
6. F. Kurie, J. Richardson, and H. Paxton, Phys. Rev. 49, 368 (1936)
7. H. A. Bethe and R. Bacher, Rev. Mod. Phys. 8, 194 (1936)
8. C. Longmire and H. Brown, Phys. Rev. 75, 264 (1949); 75, 1102 (1949)
9. S. M. Dancoff and P. Morrison, Phys. Rev. 55, 122 (1939)
10. E. Segre and A. C. Helmholtz, Rev. Mod. Phys. 21, 271 (1949)
11. P. Axel and S. M. Dancoff, Phys. Rev. 76, 892 (1949)
12. M. H. Hebb and G. E. Uhlenbeck, Physica 7, 606 (1938)
13. M. H. Hebb and E. Nelson, Phys. Rev. 58, 486 (1940)
14. M. E. Rose, G. Goertzel, B. Spinrad, J. Harr, and P. Strong, Phys. Rev. 76, 1883 (1949)
15. K. Siegbahn, Phil. Mag. 37, 181 (1946)
16. K. Siegbahn, Proc. Roy. Soc. A 188, 541 (1946)
17. M. Deutsch, W. G. Elliot, and R. D. Evans, R.S.I. 15, 178 (1944)
18. K. Siegbahn and A. Johansson, Arkiv. Mat., Astron. Fys. 34A, No. 10 (1947)
19. W. A. Higginbotham, J. Gallagher, and M. Sands, R.S.I. 18, 706 (1947)
20. G. M. Temmer, Phys. Rev. 76, 424 (1949); 76, 1002 (1949)
21. M. Lindner, Ph.D. Thesis, University of California (1948)
22. J. W. Mihelich and R. D. Hill, Bull. Am. Phys. Soc. 24, 9 (1949)
23. D. A. Lind, J. R. Brown, and J. W. DuMond, Phys. Rev. 76, 1838 (1949)
24. J. W. DuMond, D. A. Lind, and B. B. Watson, Phys. Rev. 75, 1226 (1949)
25. E. C. Crittenden, Jr., Phys. Rev. 55, 110 (1939)

26. R. A. Becker, F. S. Kirn, and W. L. Buck, Phys. Rev. 76, 1406 (1949)
27. D. R. Miller, R. C. Thompson, and B. B. Cunningham, Phys. Rev. 74, 347 (1948)
28. J. L. Lawson and J. M. Cork, Phys. Rev. 57, 982 (1940)
29. H. Bradt, P. C. Gugelot, O. Huber, H. Medicus, P. Preiswerk, and P. Scherrer, Helv. Physica Acta. 19, 77 (1946)
30. M. Deutsch and D. T. Stevenson, Phys. Rev. 76, 184 (1949) A
31. J. D. Kraus and J. M. Cork, Phys. Rev. 52, 763 (1937)
32. M. L. Poole, Phys. Rev. 53, 437 (1938)
33. G. J. Neary, Proc. Roy. Soc., 175, 71 (1940)
34. L. M. Langer and H. C. Price, Jr., Phys. Rev. 76, 641 (1949)
35. C. S. Wu and L. Feldman, Phys. Rev. 76, 696 (1949)
36. E. Feenberg and K. C. Hammack, Phys. Rev. 75, 1877 (1949)
37. A. S. Newton and W. R. McDonell, UCRL Report No. 395 (1949)
38. C. S. Wu and L. Feldman, Phys. Rev. 76, 697 (1949)
39. J. M. Cork and R. L. Thornton, Phys. Rev. 51, 608 (1937)
40. J. L. Lawson and J. M. Cork, Phys. Rev. 57, 987 (1939)
41. J. M. Cork and J. L. Lawson, Phys. Rev. 56, 291 (1939)
42. L. Seren, D. W. Engelkemeier, W. Sturm, H. W. Friedlander, S. H. Turkel, Phys. Rev. 71, 409 (1947)
43. B. Waldman, Phys. Rev. 75, 327 (1949)